Babeş-Bolyai University, Cluj-Napoca
Faculty of Biology and Geology
Department of Geology

Technological and paleoclimate reconstructions based on artifacts and sediments from archaeological sites located in caves from the Southern Carpathians

(Ph. D. Thesis Summary)

Ph.D. advisor:
Univ. Prof. Dr. Corina Ionescu

Ph.D. candidate:
Alexandra-Mihaela Enea-Giurgiu

Cluj-Napoca
2020

THESIS CONTENTS

THESIS SUMMARY CONTENTS

Keywords: ancient ceramics, Archaeometry, paleohydroclimate, carbon isotopes, Late Neolithic, Copper Age, Bronze Age, Turdaș Culture, Foeni Group, Coțofeni Culture, Great Cave of Cerișor, Cauce Cave

INTRODUCTION

Archaeological sites provide valuable materials, such as *artifacts* and *sediments*, which can help to decipher and reconstruct the behavior of prehistoric people. Migration, social life, technological knowledge, interactions between populations, possible trading routes, environment and climate in which people lived, chronologies, decline or flourishing of a civilization can all be inferred after studying the artifacts and sediments with appropriate methods.

Sediments are composed of particles with various sizes, which may consist of various minerals, rock fragments, fossils, charcoal, guano and plant remains. They are widely used for past climate studies, for determination of ancient human activities or for chronology (Hall et al., 2008; Masi et al., 2013; Kanthilatha, 2016). Charcoal is commonly encountered in lake deposits, peat bogs or guano deposits and is widely used to infer past fire regimes (Feurdean & Vasiliev, 2019; Florescu et al., 2019). It is also well preserved in many archaeological sites. When recovered from hearths, it indicates the deliberate use of fire (Cohen-Ofri et al., 2006) and provides absolute ages through radiocarbon dating (Scott & Damblon, 2010). Several studies (Ferrio et al., 2006; Hall et al., 2008; Masi et al., 2012; Audiard et al., 2019) have shown that the climatic signal of wood $\delta^{13}C$ is preserved in charcoal and, consequently, rainfall, humidity and temperature for past times can be derived. However, studies using $\delta^{13}C$ to infer these parameters are scarce and have not been carried out on charcoal from Romanian sites.

From Holocene archaeological sites, regardless of their location (caves or surface), the most abundant artifact which is usually unearthed are made of ceramic material. Ceramics is known for its high resistance to alteration (including burial for long periods of time) due to special physical and chemical characteristics (Maritan, 2004; Ionescu & Hoeck, 2011; Hunt, 2017). The ceramic product is regarded as an ‘artificial rock’ (Maggetti, 1982, 2001) formed through anthropogenic pyrometamorphism at atmospheric pressure (Grapes, 2011). A huge number of sherds were excavated over time from surface or cave sites in Romania, but many

finds lack complex studies which could reveal the technological processes involved in ceramics making, the composition of the paste, the provenance of raw materials and the firing conditions. Still, the existing studies highlighted the variety of processes involved in ceramic production. They also point to the need of increase of such studies to fill the gaps in this field.

Considering the above discussion, the archaeological sites located either at the surface or in caves/rock shelters are widespread and contain valuable finds and sediments. Finds from caves are particularly important as they may reflect a permanent or temporary settlement (Roman, 1976; Mentzer, 2017). Caves were places where people stored or produced artifacts. Temporary use might have been related to various activities such as hunting, plant gathering, transhumance or sheltering in times of danger (Mavridis et al., 2013). From archaeological point of view, caves act to a certain degree as closed systems, meaning that what gets inside, will usually remain inside, affected only by post depositional transformations (Karkanas & Goldberg, 2019). In Romania, Boroneanț (2000) has described more than 250 caves containing archaeological remains. Still, the real number remains unknown and the ceramic artifacts provided by cave sites are understudied from an archaeometric point of view. Also, archaeological charcoal was mainly used for radiocarbon dating, but remains insufficiently exploited as it regards the $\delta^{13}C$ values and related outcomes (*e.g*. inferring the humidity) (see Hall et al., 2008; Masi et al., 2012, 2013).

The present study includes two archaeological sites located in caves from the Poiana Ruscă Mountains (Southern Carpathians, Romania). The caves, namely the Great Cave of Cerișor ("Peștera Mare de la Cerișor", *in Romanian*) (hereafter GCC) and the Cauce Cave ("Peștera Cauce", *in Romanian*) (hereafter CC) are rich in archaeological findings such as lithic tools, adornments and ceramics, as well as anthropogenic charcoal (Roman et al., 2000; Luca et al., 2004, 2005). The analysed c*harcoal* fragments were collected from both cave sediments and hearths. Additionally, *potsherds* from the Great Cave of Cerișor have been selected for investigation. Archaeologically, the potsherds are assigned to the Late Neolithic Turdaș Culture (ca. 4,950–4,550 B.C.), Early Eneolithic Foeni Group (ca. 4,700–4,450 B.C.) and the Copper Age Coțofeni Culture (ca. 3,500 – 2,500 B.C.). These populations occupied significant areas on the present-day territory of Romania, e.g., Turdaș remains are known from 74 sites, Foeni artifacts were recovered from 28 excavations, whereas Coțofeni culture was described from more than 688 sites (Ciugudean, 2000; Diaconescu, 2014; Bințințan & Gligor, 2016).

First results obtained on two sets of potsherds (assigned to the Foeni Group and the Coțofeni Culture) found in the Great Cave of Cerișor were published by Giurgiu et al. (2017b, 2019) and their detailed study is displayed in Chapter 5. Data presented at various scientific meetings (*e.g.* Enea-Giurgiu et al., 2018, 2019; Giurgiu et al., 2016ab), are also included in this study.

GEOLOGICAL SETTING AND CAVE DESCRIPTION

Geographically, both the Great Cave of Cerișor and the Cauce Cave are in the Poiana Ruscă Mountains, Romania (Fig. 1). Geologically, the area is assigned to the Getic Domain of the Southern Carpathians, a 300 km-long mountain belt consisting of Paleozoic and Proterozoic basement rocks, Mesozoic sequences, and Cenozoic sedimentary cover (Mureşan et al., 1980; Iancu et al., 2005a; Balintoni et al., 2011).

The polyphasic tectonic evolution of the Southern Carpathians resulted in a complex structure which was described and discussed in many studies (*e.g*. Balintoni, 1997; Iancu et al., 2005ab; Balintoni et al., 2011). Three main nappe complexes were separated: Getic-Supragetic basement/cover nappe complex at the top, the Severin cover nappes in the middle, and the Danubian basement/cover nappe complex at the bottom, respectively. Except for the Severin cover nappes which have an oceanic origin, the rest of the nappe stacks have a continental nature. The nappe structure of the Southern Carpathians was defined in the Cretaceous times, during two major events, namely the "Austrian phase" (Mid-Cretaceous) and the "Laramide phase" (Late Cretaceous) (Iancu et al., 2005a).

The Great Cave of Cerișor (coordinates: N45º45'7.74" E22º46'18.54"; 580 m a.s.l.) and the Cauce Cave (coordinates: N45º45'40.56" E22º45'6.48"; 670 m a.s.l.) open on the southern flank of the Runc Valley, in the rocks of the *Hunedoara-Luncani Formation* (Balintoni, 1997) which is a Mid-Paleozoic carbonatic sequence (limestones and dolomites).

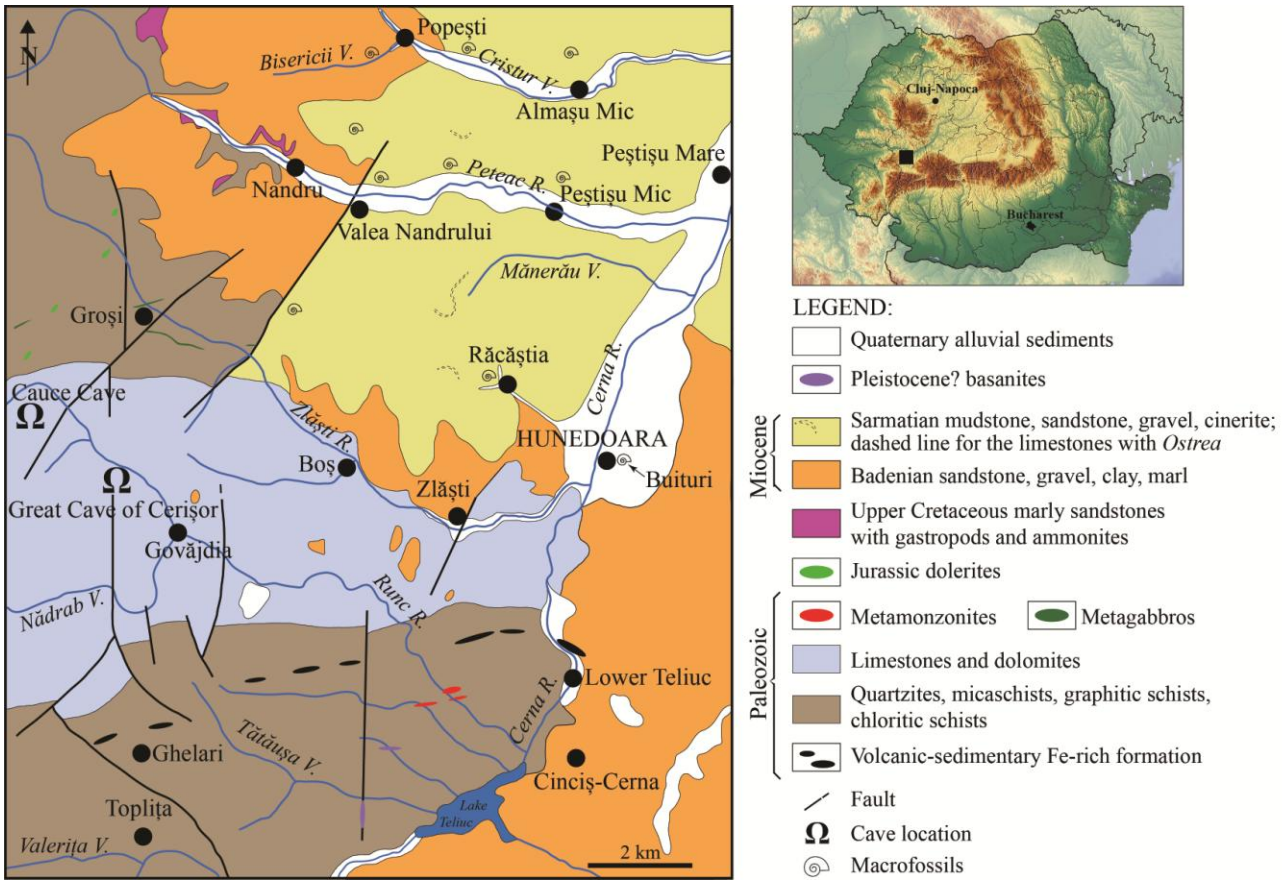

Fig. 1. Modified geological map from Giurgiu et al. (2017b, 2019), based on Mureşan et al. (1980), with the location of the 'Great Cave of Cerişor' and the 'Cauce Cave' in the Poiana Ruscă Mountains (Southern Carpathians). The upper right insert shows the position of the map within Romania.

ARCHAEOLOGICAL BACKGROUND

Stratigraphy of the Great Cave of Cerişor. Based on ceramic artifacts exhumed at the GCC, several cultural groups and related ages were defined (Boroffka, 1995; Roman et al., 2000): the Turdaș – Late Neolithic, the Foeni Group – Early Eneolithic, the Coțofeni – Copper Age (Chalcolithic), and the Wietenberg Culture – Middle Bronze Age. At the top of stratigraphy mixed materials from VIII-IXth, XI-XIIIth and post-XVth centuries were found, but the pieces are isolated and there are no complexes or specific levels in the stratigraphy of the cave to demonstrate a long habitation during the middle ages (Roman et al., 2000). The potsherds assigned to the Turdaș, Foeni Group and Coțofeni cultures are included in this study and their particularities will be further discussed. A profile located in the archaeological excavation S1

from the Great Cave of Cerișor was investigated. The deposit is 49 cm thick and consists of thin layers of silt and clay, with carbonate fragments.

Stratigraphy of the Cauce Cave. At the Cauce Cave several levels were described by Luca et al. (2004). The profile starts with Starčevo-Criș (Neolithic) Culture, followed by a level with Turdaș (Late Neolithic) finds which also contains few Foeni (Early Eneolithic) and Petrești Culture (Eneolithic) ceramic at the top. The next layer belongs to Tiszapolgár Culture and contains Hunyadihálom (Copper Age) artifacts at the upmost part. The following levels contain Coțofeni (Copper Age), Wietenberg (Bronze Age) and, at the end of the succession, medieval materials. The culture assignment is based on the archaeological finds, mostly pottery. The investigated succession is 110 cm deep and consists of silt and clay.

Turdaș Culture. The Late Neolithic Turdaș archaeological sites are spread in the western and southwestern parts of the Transylvanian Basin, as well as along the Mureș Valley up to the western part of the Romanian territory. There are 74 sites which contain Turdaș archaeological finds (Diaconescu, 2014) among which the type locality where this culture features have been defined (Luca et al., 2004). Based on radiocarbon dating, the Turdaș Culture lasted from around 4,950 (in the so-called "Vinča-C2 phase") till around 4,550 B.C. when the population of the Foeni Group arrived in Transylvania (Drașovean, 2013; Diaconescu, 2014).

Foeni Group. The Early Eneolithic Foeni population appeared firstly in the southwestern part of the present-day territory of Romania (Banat) and later spread in the Transylvania area. The radiocarbon dating indicates a time span between ~4,700 and ~4,450 B.C. (Drașovean, 2013; Gligor, 2014). This population significantly contributed to the genesis of the two well-known Copper Age cultures within Romania, namely the Cucuteni and the Petrești cultures (Luca et al., 2004; Drașovean, 2013; Gligor, 2014). Up to now, 28 Foeni archaeological sites have been investigated, the most important being those at Alba Iulia, Daia Română, Mintia, Petrești, and Cauce Cave (Gligor, 2008; Bințințan & Gligor, 2016).

Coțofeni Culture. Between ~3,500 and ~2,500 cal. B.C., the Copper Age Coţofeni Culture occupied a large territory in the south-west, west and central parts of the present-day

Romania, *i.e.*, Banat, Oltenia, W Muntenia, Crişana, and Transylvania (Forenbaher, 1993; Ciugudean, 2000; Lazarovici & Lazarovici, 2007; Boroffka, 2013). Remnants of this culture were also found in NE Serbia and NW Bulgaria (Roman, 1976; Spasić, 2010). Ciugudean (2000) mentions 688 documented archaeological sites in Transylvania and Banat with Coțofeni finds, but he considers the real number to be higher.

PALEOCLIMATE RECONSTRUCTION

Introduction

Sediments which are produced or affected by human activities are defined as "anthropogenic sediments". In archaeological sites, they usually comprise charcoal, ash and other organic materials intentionally brought by people to the site. Charcoal and ash are the by-products of wood burning and in archaeological sites are commonly found associated with combustion features, such as hearths[1] and hearths areas (less intact fire-related features) (Dibble et al., 2009). Generally, charcoal[2] is defined as a solid material resulted through the process of pyrolysis (Cohen-Ofri et al., 2006; Bird & Ascough, 2012). It is a form of charred material produced by burning of wood in natural fires or fires related to human activities. Carbon is the major element of charcoal and this topic will be addressed below.

Carbon is the major component of charcoal and has three isotopes[3]. One carbon isotope (^{14}C) is unstable (radioactive), and two (^{12}C and ^{13}C) are stable. The unstable nuclide (^{14}C) is used in radiocarbon dating, the method being suitable to samples with ages up to ~50,000 ^{14}C years before present (BP) (Bird & Ascough, 2012; Wagner et al., 2018).

The stable isotopes (^{12}C and ^{13}C) are measured as a ratio ($^{13}C/^{12}C$) and are reported in the delta notation ($\delta^{13}C$) relative to an international standard with a known isotope ratio, *e.g.* the Vienna Pee Dee Belemnite (VPDB) standard, and expressed in per mil (‰) (Coplen, 1996; Bird & Ascough, 2012; Tiwari et al., 2015; Wagner et al., 2018). Relative to VPDB standard, the $\delta^{13}C$ values are expressed as follows: $\delta^{13}C = [(R_{sample}/R_{standard}) - 1] \times 1000$ (‰), where R represents the

[1] Remnants of domestic fire which are intact or preserve most of the original compositional elements such as organic matter and ash (Dibble et al., 2009).
[2] Also known as pyrogenic carbon, char, black carbon or soot (Bird & Ascough, 2012).
[3] Isotopes are atoms of an element which have the same number of protons but different number of neutrons, *i.e.*, they have same atomic number but different mass number (Tiwari et al., 2015; Wagner et al., 2018).

measured $^{13}C/^{12}C$ ratio of the sample and standard, respectively. They are commonly used to infer past environmental conditions (Kohn, 2010; Kohn, 2016).

Photosynthetic pathways. Based on the photosynthetic mechanism used for CO_2 fixation from the atmosphere, the terrestrial plants are divided into three categories: C_3 (using the Calvin cycle), C_4 (using the Hatch–Slack pathway) and CAM (crasulacean acid metabolism) plants. C_3 plants grow well in temperate climates, but are found both in the warmest deserts, and in the coldest arctic environments. C_4 plants (about 3% of terrestrial plants) are abundant in grasslands from the tropical, subtropical, and temperate zones with a high intensity of the light, high temperatures and summer rains. They are rare or absent in cold environments. CAM plants account for 7% of all vascular plant species and grow in stressful environments (Bräutigam et al., 2017). CAM plants such as cactuses easily adapt to extreme arid conditions, but have a very low photosynthetic capacity. Conversely, the C_4 plants are adapted to strong light, as well as arid and warm environments and have a higher photosynthetic capacity compared to C_3 plants.

Isotopic fractionation. The differences in the biochemistry and physiology of C_3, C_4 and CAM photosynthetic pathways lead to different carbon isotopic fractionation and are reflected by the $\delta^{13}C$ values. For the terrestrial plants, the isotopic composition ranges between −8‰ and −34‰. The most important differences occur as result of isotope fractionation during photosynthesis (Bird & Ascough, 2012). During photosynthetic CO_2 fixation, the fractionation of carbon isotopes determines the depletion of the heavier ^{13}C isotope in plants (because ^{13}C reacts slower than ^{12}C) (Brugnoli & Farquhar, 2000).

The plants using the C_4 pathway have higher $\delta^{13}C$ values (−10 to −14‰), showing a smaller isotope fractionation (O'Leary et al., 1992). The CAM plants show a wide range of $\delta^{13}C$ values, intermediate between those of the C_3 and the C_4 plants (Osmond et al., 1973). The C_3 plants use the more ^{13}C discriminating pathway (*i.e.* a larger fractionation, of about −18‰, occurs). They have low $\delta^{13}C$ values, ranging between −20 and −37‰ (Kohn, 2010), with an average of −27‰ (Van Klinken et al., 1994; Cerling et al., 1997). Variations of the fractionation process during the photosynthesis occur in C_3 plants and are influenced by the differences in water use efficiency, light use, CO_2 recycling and other factors. The atmospheric CO_2 concentration and precipitation influence the water use efficiency (Silva & Horwath, 2013). Plant

$\delta^{13}C$ also depends on the mean annual precipitation (MAP), but show negligible dependency of p_{CO2} (Kohn, 2016). The indigenous vegetation from the area where the caves are located belongs to the C_3 type and the fractionation associated with C_3 photosynthetic mechanism will be considered in this study.

Charcoal $\delta^{13}C$. The factors that yield variation in charcoal isotope composition are represented by: (i) the increasing burning temperature and (ii) the isotopic value of the original wood (Hall et al., 2008). The first factor influencing the $\delta^{13}C$ values is the combustion temperature. Several studies (Turney et al., 2006; Hall et al., 2008) have shown that the $\delta^{13}C$ values for charcoal are more negative compared to the source material. The experimentally-obtained charcoal is depleted in ^{13}C, demonstrating that the fractionation increases with temperatures up to 550 °C (Turney et al., 2006; Audiard et al., 2019) and ranges between 1 and 1.3 ‰ (Turney et al., 2006). Ferrio et al. (2006) have described pyrolysis-induced $\delta^{13}C$ shifts of up to 1‰ at a temperature of 550 °C in average. The duration of the wood heating at a specific temperature does not significantly influence the isotopic composition, the charcoal composition becoming stable after 30 minutes of heating (Turney et al., 2006). Other experimental studies showed no significant isotopic change after equilibration (Schleser et al., 1999; Krull et al., 2003) or only a 1–2‰ increase (Turekian et al., 1998; Poole et al., 2002). Regardless the increase/decrease of the isotopic values in charcoal, the literature data clearly indicates that char retains the environmental signal recorded during the growth of the tree and can be used for paleoclimate reconstructions with a proper handling (Ferrio et al., 2006).

Present-day climate and vegetation

The climate of the Romanian Carpathians according to Micu et al. (2015) is moderately humid with the wettest areas being represented by the Southern and Apuseni Mountains. They also mention that at altitudes up to 800 m the mean annual precipitation is around 800 mm. According to CarpatClim (http://www.carpatclim-eu.org/) the study area falls within the regions with 700-800 mm of mean yearly precipitation (based on processed data between 1962 and 2010). Processed data for the year 2010 from CarpatClim atlas shows that the caves are located in an area with an average of 800 mm annual precipitation.

The vegetation close to the region where the caves are located (*i.e.* at ~22 km south from

the caves) is represented by forests with *Quercus petraea* and *Carpinus betulus* or hornbeam mixed with *Fagus sylvatica*. Rarely, *Abies alba* and *Picea abies* occur. *Quercus* is found along Runc Valley, especially on the southern part of its left flank. Other shrubs in the area comprise *Corylus avellana*, *Cornus mas* and *Crataegus monogyn*a (Rusu, 1998). The Cerișor–Lelese plateau is characterized by meadows with Poaceae (Chirică & Răceanu, 1976). The Rosaceae and the Ericaceae are common (Filipaș et al., 2013). Near the entrances of the caves, mosses (*Sphagnum*) and *Fagus* are abundant (genus determined by Dr. I. Tanțău, Babeș-Bolyai University).

Samples and analytical methods

The Great Cave of Cerișor. The radiocarbon dating was carried out on three charcoal samples (labeled PC3, PC8, PC38) taken from the hearths or charcoal-rich levels of the Late Neolithic, Eneolithic and Bronze Age sediments. For the $\delta^{13}C$ measurements, eight charcoal samples were collected from a 49 cm thick sequence.

The Cauce Cave. For the radiocarbon dating, four charcoal (labeled CAU1, CAU2, CAU3, CAU5) samples from Late Neolithic, Eneolithic and Bronze Age levels were sampled. For the $\delta^{13}C$ measurements, twelve charcoal samples were recovered from hearths as well as from the rest of the sediments composing the 110 cm depth sequence.

Radiocarbon dating. The ^{14}C dating of the charcoal samples from the Great Cave of Cerișor was performed at the Poznań Radiocarbon Laboratory (Poland) using accelerator mass spectrometry (AMS). The charcoal from the Cauce Cave was dated by AMS at the RoAMS Laboratory of the Horia Hulubei National Institute for R&D in Physics and Nuclear Engineering (Măgurele, Romania). For generating the deposition model for each profile, the OxCal 4.3.2 software (Bronk Ramsey, 2017; Bronk Ramsey & Lee, 2013) was used. The calibration of the ^{14}C dates was performed using the IntCal13 (Reimer et al., 2013) calibration curve.

Stable isotopes measurements. After sample preparation, for measuring the isotopic $\delta^{13}C$ values, a combustion module from Costech Analytical Technologies Inc. coupled to a Picarro Cavity Ring Down Spectroscopy G2121-i analyzer (Busch & Busch, 1999; Berden & Engeln,

2009) from the Stable Isotope Laboratory of the Babeș-Bolyai University (Cluj-Napoca, Romania) were used. All $\delta^{13}C$ values are expressed relative to VPDB.

Results and discussions

Radiocarbon ages. In order to check the certainty of the ^{14}C results, the radiocarbon dates from GCC and CC were compared to existing absolute ages from other archaeological sites (Table 1). Establishing other details (*e.g.* the start/end of a culture/group) was not the purpose of this study and the comparison strictly intends to establish whether the obtained dates from this study are feasible or not.

Table 1. Ages from other studies used for comparison.

Locality	Culture/Group	Age (BP)	Error	Lab code	Source
Orăștie	Turdaș	6070	70	Deb-5765	Luca (2001)
Orăștie		5825	60	Deb-5762	Luca (2001)
Orăștie		5790	55	Deb-5775	Luca (2001)
Cauce		5760	40	GrN-28994	Luca (2009)
Foeni	Foeni	5890	40	Poz-53356	Drașovean (2013)
Foeni		5855	85	Deb-5771	Drașovean (2004)
HD		5820	35	Poz-56766	Tincu (2015)
Alba Iulia *Lumea Nouă*		5770	40	Poz-19377	Gligor (2009)
Foeni		5750	40	Poz-53388	Drașovean (2013)
Hunedoara		5730	35	Poz-58370	Tincu (2015)
Barca Baloty	Hunyadihálom	5074	27	MAMS-14250	Brummack (2015)
Barca Baloty		5096	27	MAMS-14252	Brummack (2015)
Tiszalúc-Sarkad		5020	40	Poz-36362	Raczky-Siklósi (2013)
Tiszalúc-Sarkad		5050	40	Poz-36363	Raczky-Siklósi (2013)
Tiszalúc-Sarkad		5070	40	Poz-36361	Raczky-Siklósi (2013)
Silvașu de Jos	Coțofeni	4430	50	Poz-56674	Diaconescu & Tincu (2016)
Băile Herculane		4360	50	LJ-3534	Bojadžiev (1998)
Băile Herculane		4350	60	LJ-3535	Bojadžiev (1998)
Ostrovu Corbului		4400	60	LJ-3799	Ciugudean (2000)
Sebeș	Wietenberg	3495	40	AA-103619	Bălan et al. (2016)
Sebeș		3501	40	AA-103620	Bălan et al. (2016)
Sebeș		3555	41	AA-103615	Bălan et al. (2016)
Oarța de Sus		3507	37	Bln-5626	Kacsó (2004)

The Late Neolithic. A ^{14}C dating for the Turdaș Culture from the Cauce Cave was previously carried out on a bovidae tibia (Luca, 2009), but its accuracy was questioned because of controversies related to the sampling depth (Diaconescu, 2014). The resulted age was 5,760 ± 40 B.P. (Luca, 2009) and is strikingly conformable with the age obtained in the present study for the Turdaș layer from The Great Cave of Cerișor (sample PC3: 5,740 ± 40 B.P.). However, until a clarification of the context from which the sample dated by Luca (2009) was taken (*i.e.* establishing the precise location within the Cauce Cave profile and determination of the

postdepositional processes which could have affected the sample and/or the site), it can be stated that the obtained value fits with a Turdaș inhabitance strictly from a numerical point of view, but cannot be considered a reliable result.

The sample from the deepest GCC layer (*i.e.* sample PC3, from the layer containing Turdaș Culture and Foeni Group sherds) fits well with the ages obtained for the Turdaș Culture from Orăștie (Luca, 2001, 2009). Also, the age obtained from sample PC3 matches also the ages for the Foeni Group obtained from the Foeni village, as well as the Hunedoara and Alba Iulia cities (Luca, 2001; Gligor, 2009; Drașovean, 2013; Tincu, 2015). The ^{14}C dates obtained in this study for the Turdaș layer (with Foeni potsherds at the top) from the Cauce Cave are older than the one obtained for Turdaș sample from GCC profile. Still, they correlate well with the Turdaș Culture ages from Orăștie and with the Foeni Group ages from Foeni archaeological site.

Overall, compared with the ^{14}C values from literature and taking in consideration the relative age inferred by the potsherds, the absolute ages obtained for the PC3, CAU1 and CAU2 sample are trustworthy. These ages, close to those of the Foeni group, are not surprising as the two populations are known to have intersected.

The Copper Age. The sample CAU3 (5,034 ± 30 B.P.) was taken from a Copper Age layer situated at 79 cm below surface in the Cauce Cave profile. The sediments from this layer were attributed to the Tiszapolgár Culture. However, this layer was also mentioned as having Bodrogkeresztúr III ("Toarte pastilate" type pottery or 'Hunyadihálom') potsherds at the top (Luca et al., 2004). The calibrated date for sample CAU3 (5,897–5,710 cal B.P., 2σ) fits best with the radiocarbon dates of the 'Lažňany–Hunyadihálom group 'summarized by Brummack & Diaconescu (2015). These authors also proposed an occurrence scheme in which Tiszapolgár Culture is followed by Bodrogkeresztúr Culture. Hunyadihálom culture would be the last in this timeline. The obtained date marks the existence of a Hunyadihálom population in the Cauce Cave and it correlates well with the dates from Tiszalúc-Sarkad (Hungary) and Barca Baloty (Slovakia) sites (Rackzy & Siklósi, 2013; Brummack & Diaconescu, 2015; Brummack, 2015).

The sample PC8 (4,370 ± 35 B.P.) was recovered from another Copper Age layer, namely the Coțofeni Culture. The charcoal was sampled from GCC profile from a depth of 41 cm below surface and provided an age of 4,987–4,855 cal B.P. (2σ), which correlates with the Coțofeni ages from Băile Herculane, Ostrovu Corbului and Silvașu de Jos sites (Roman, 1976;

Forenbaher, 1993; Ciugudean, 2000; Diaconescu & Tincu, 2016).

The Bronze Age. Both sites (GCC and CC) contain Bronze Age layers containing Wietenberg Culture artifacts. The age from GCC is 3,856–3,686 cal B.P. for sample PC38 (taken from the middle of the Bronze Age layer), whereas the CAU5 (sampled from the base of the Bronze Age layer) from CC provided an age of 3,991–3,849 cal B.P. Overall, the results fit with the ^{14}C data obtained from Sebeș and Oarța de Sus sites for Wietenberg Culture (Kacsó, 2015; Bălan et al., 2016).

Age-depth models. At GCC, the chronology of the interval from 17 cm to 46 cm in the profile is based on three charcoal samples which returned ages in stratigraphic order. The ages cover an interval of ~2,750 years, between 6,440 cal B.P. and 3,686 cal B.P. In the lowest part of the succession, between 6,440 cal B.P. (Late Neolithic) and 4,855 cal B.P. (Cooper Age), the sediments accumulated at low rates, resulting in a 5 cm thick layer. At 4,855 cal B.P. an increase of the deposition rate is observed and is maintained until at 3,686 cal B.P. (Bronze Age).

In the Cauce Cave, the chronology for the interval between 42 cm to 104.5 cm in the profile is based on four charcoal samples which returned ages in stratigraphic order. The ages span an interval of ~2,790 years, between 6,658 cal B.P. and 3,850 cal B.P. As in the case of GCC, a deposition model was simulated for the dated part of the profile. In the lowest part of the profile, the samples CAU1 and CAU2 have very close ages (6,658 cal B.P. and 6,560 cal B.P., respectively). In between these samples, there is an 11.5 cm thick layer of sediments which accumulated rapidly. From 6,560 cal B.P. (sample CAU2, Late Neolithic) to the upmost ^{14}C dated sample (Bronze Age), the sedimentation rate constantly decreased.

Charcoal $\delta^{13}C$. For GCC, charcoal $\delta^{13}C$ values range from –27.63 to –21.76‰, with an average of –24.38 ‰. The carbon isotopic record shows a noticeably increase at the depths of 28 cm and 36.5 cm, reaching values of –22.17‰ and –21.76‰, respectively. The corresponding age interval when this variation occurs is between 4,199 cal B.P. and 4,699 cal B.P. Except of this shift, the $\delta^{13}C$ values show a negative trend, with the most depleted charcoal having a value of –27.63‰. *For CC*, the charcoal $\delta^{13}C$ values vary from –26‰ to –22.99‰, with an average of –24.48‰. The results show three moments, with a significant increase of the isotopic values. The

first variation was recorded in the charcoals from the depth of 50 cm and 54 cm and is illustrated by values of –22.99‰ and –23.07‰, respectively. The time span during which this variation persisted is between 4,242 cal B.P. and 4,439 cal B.P., as inferred from the deposition model. The second shift towards higher values is documented by charcoals from the depths of 75 cm and 79 cm. The corresponding $\delta^{13}C$ values for these depths are –23.51‰ and –23.71‰, respectively, and they are recorded in the time interval ranging from 5,469 cal B.P. to 5,665 cal B.P. The last variation occurs at the depth of 95 cm where the charcoal had a $\delta^{13}C$ value of –23.73‰ (corresponding age from the age-depth model: 6,577 cal B.P.).

Environmental changes inferred from $\delta^{13}C$

Numerous studies have used the $\delta^{13}C$ of plants to describe the past hydroclimate of a region, whereas other studies have interpreted the $\delta^{13}C$ values as indicators of a shift between C_3 and C_4 plants (see Onac et al., 2014; Forray et al., 2015; Campbell et al., 2017; Cleary et al., 2019). In recent studies, the $\delta^{13}C$ from fossil charcoal has been proved to represent the paleoclimatic signal and was subsequently used to describe past climate changes (see *e.g.,* Ferrio et al., 2006; Hall et al., 2008; Aguilera et al., 2009, 2012; Masi et al., 2012, 2013; Baton et al., 2017; Audiard et al., 2019).

The obtained $\delta^{13}C$ data for GCC and CC all within the range of −20 and −37‰ specific to the C_3 plants (Kohn, 2010), pointing to a charcoal formed from a woody plant using the C_3 pathway. In order to infer the environmental conditions for the studied time span, the measured $\delta^{13}C$ values were compared with existing isotopic data from other records.

Generally, for the time interval between 6,658 cal B.P. and 3,642 cal B.P. inferred from the ^{14}C datings, the vegetation at altitudes such as those characteristic to the study area consisted of mainly *Carpinus betulus*, *Corylus*, *Quercus*, *Tilia*, *Fraxiuns* and *Picea*, with a shift to *Fagus sylvatica* towards the end of the interval. Similar vegetation trends were described based on two sequences from Avrig (Tanțău et al., 2006). The first climatic variation occurs at ~6,500 cal B.P. when the isotopic data from Cauce Cave points to a wetter period (*i.e.* lower $\delta^{13}C$ values) compared with the preceding times. The isotope values from Cauce Cave show an increase from ~ 6,500 cal B.P. until ~5,500 cal B.P. Currently, the charcoal $\delta^{13}C$ documents a dry event (*i.e.* higher $\delta^{13}C$ values), which correlates with the oxygen data from PU-2 and GISP2. The stalagmite and ice core oxygen data suggest a warm climate, but from ~5,500 cal B.P. the

temperatures start to deteriorate (Onac et al., 2002). A return to wetter conditions is indicated by the $\delta^{13}C$ values at 4,750 cal B.P., but shows no correspondence in the graphs of PU-2 or GISP2. However, the data from Poleva Cave indicate slightly warmer conditions.

The most dramatic climate change recorded by the $\delta^{13}C$ data occurs at 4,250 cal B.P. A sharp increase of $\delta^{13}C$ values from GCC and CC is visible, pointing to a dry event just before the Bronze Age inhabitance. The carbon isotopes from PU-2 also increase, indicating aridity. The dry spike from Cauce Cave correlates (slightly shifted) with the trends shown by the oxygen isotope data from GISP2 and PU-2. The cold and drought conditions inferred from the charcoal $\delta^{13}C$ for the 4,200 cal B.P. are supported by the vegetation described from Iaz and Avrig sites (Tanțău et al., 2006, 2016). After the 4,200 cal B.P. event, the climate documented from Cauce Cave becomes more humid, correlating with data from PU-2. At Avrig, the *Fagus* pollen values also increase after 3,880 cal B.P., indicating a switch to a moist and cold environment and similar vegetation (with the spreading of *Fagus sylvatica*) and environmental conditions were described from Iaz (Tanțău et al., 2006, 2016).

The aridity episodes from GCC and Cauce Cave also correlate well with archaeobotanical remains $\delta^{13}C$ records from other sites in Europe. In Turkey, Masi et al. (2013) have described the paleohydroclimate for the ~5,300 and 3,950 cal B.P. interval using $\delta^{13}C$ measured from archaeological charcoal and the data indicated dryness around 5,300 cal B.P. and 4,250 cal B.P. Similar drought episodes were found by Aguilera et al. (2012) from $\delta^{13}C$ of archaeological charcoal and cereal grains recovered from the Iberian Peninsula.

Across the globe, data from other ahrchives recognize the existence of a cold period around 4,200 cal B.P. (the so-called "4.2 ka event") which was mostly dry (Perry & Hsu, 2000; Margaritelli et al., 2016; Weiss, 2016; Schirrmacher et al., 2020). In 2018 it has been accepted as boundary between the 'Meghalayan stage' (Late Holocene) and 'Northgrippian' (Middle Holocene).

The results from Great Cave of Cerișor and Cauce Cave add up to the few previous studies which demonstrated the possibility of inferring paleohydrological conditions using the $\delta^{13}C$ data obtained from archaeological charcoal. The presented approach provides a basic model of how archaeological charcoal can be used to infer the paleohydroclimate, especially in areas where other climate archives lack. The study is unique on the Romanian territory, pointing to the need of further research using the charcoal $\delta^{13}C$ as proxy.

CERAMICS

Introduction[4]

The ceramic body consists of a matrix (groundmass) which embeds various-sized clasts and firing phases (Magetti, 1982; Ionescu & Ghergari, 2007; Ionescu & Hoeck, 2017). Apart of clasts, the sherds contain various voids. The surface can be covered by slip, paint, or glaze. During burial, secondary mineral products may form either through contamination for the surrounding environment or through the transformation of the initial components. The *matrix* is an inhomogeneous mixture of particles with dimensions under 15 μm (Maggetti, 1979) or under 20 μm (Ionescu & Ghergari, 2007) which are thermally transformed. Depending of the firing temperature, the optical character of the matrix ranges from birefringent to isotropic. A low crystallinity degree corresponds to a high firing temperature. *Clasts* are aplastic components which originate from the temper and to a less extent from the raw clays. The temper is added for plasticity control and has a role in preserving the form of the object after modeling. *Fabric* is a term that includes the structure and the texture of the ceramic body. The former refers to fineness (granulometry) and is described using the Wentworth scale. The latter, refers to the spatial arrangement of the components, especially of the elongated ones such as micas and pores (Ionescu & Ghergari, 2007). Therefore, the texture can be not-oriented (no arrangement of elongated elements), oriented (preferential alignment parallel to the ceramic wall) or mixed (a combination of unoriented and oriented texture).

Samples and analytical methods

Ceramic samples. Two hundred sixty-four ceramic potsherds excavated in the Great Cave of Cerișor were studied. They are assigned to the Turdaș Culture, the Foeni Group, and the Coțofeni Culture.

The Late Neolithic Turdaș samples studied here includes twenty semifine and fine ceramic sherds. Seven Foeni Group potsherds fine ceramic sherds assigned to the Early Eneolithic Foeni Group (by Dr. C. Roman and Dr. S. Tincu, firstly mentioned in Giurgiu et al. (2019)) were studied. The sherds were found in the same stratigraphic level as the Turdaș

[4] This chapter follows the Archaeoceramic course teached by C. Ionescu at the Babes-Bolyai University Cluj-Napoca, as well as within the ERASMUS program Chermat (Paris Marne-la-Valee).

materials (Roman et al., 2000). The number of potsherds assigned to the Copper Age Coțofeni Culture is much higher (237 pieces) compared to the Foeni Group and Turdaș ones. Macroscopically, the fineness is medium to coarse.

Geological samples. In order to compare the cave ceramic finds with potential raw materials, a total of 14 samples (Table 2) consisting of Quaternary sediments from the GCC cave as well as Miocene mudstones and sandstones cropping out in the area were analyzed.

Table 2. Characteristics of the geological samples.

Outcrop	Location/GPS	Samples		Depth (cm)	Lithology of the outcrop
		Label	Description		
GCC	Entrance 2	CER-1	Sandy clays	0-10	Light orange clays with large carbonate rock fragments and sand
	S1 archaeological trench	CER-2	Sandy clays	20	Orange clays with centimetric carbonate rock fragments and sand
Outcrop I	Peteac Valley 45°48'5.64"N, 22°49'55.38"E	CER-3	Mudstone	0-10	Gray mudstone with thin layers of orange sand
		CER-4	Mudstone mixed with sand	30	
Outcrop II	Peteac Valley 45°48'6.78"N, 22°50'9.36"E	CER-5	Marl	0	Cream-colored marl with fossils
Outcrop III	Peteac Valley 45°48'4.44"N, 22°50'19.56"E	CER-6	Mix of clays and sand	123	Yellowish-cream mudstones alternating with orange sandstone layers
		CER-7		130	
		CER-8		155	
		CER-9		190	
		CER-10		250	
		CER-11		270	
		CER-12		290	
		CER-13		300	
Outcrop IV	Quarry, S of Hunedoara 45°44'29.2"N 22°54'14.9"E	CER-14	Mix of sandstone and mudstone	53	Alternation of cream-colored sandstone and thin orange or gray mudstone

Analytical methods. Two hundred sixty-four ceramic potsherds assigned to the Turdaș Culture, Foeni Group and the Coțofeni Culture were investigated by polarized light optical microscopy (OM), X-ray powder diffraction (XRPD), electron microprobe analysis and scanning electron microscopy (SEM), as presented in Table 3. The geological samples were analyzed by X-ray powder diffraction (XRPD).

Table 3. Potsherds samples and type of analysis performed on each culture/group.

Culture/ Group	Total no. of sherds	Sherd number	Analytical methods			
			OM	XRPD	EMPA	SEM
Foeni	7	CE-77 to CE-83	7 samples	7 samples	2 samples	3 samples
Turdaş	20	CE-67 to CE-76 CE-255 to CE-264	20 samples	20 samples	2 samples	-
Coțofeni	237	CE-1 to CE-66 CE-84 to CE-254	237 samples	80 samples	4 samples	2 samples

Results

Geological samples. The Miocene mudstones sampled from outcrop III have similar mineralogical composition (Table 4), with the predominance of quartz, illite/muscovite, and feldspars. The wide peak at 14 Å could have been produced by both chlorite and smectite. The shift of this diffraction peak from 14 Å to 17 Å in a glycolated sample (CER-11) proves the presence of smectite (probably montmorillonite). The lack of a 14 Å diffraction peak after glycolation indicates the absence of chlorite.

Table 4. Mineralogy of the geological samples, obtained by XRPD. Abbreviations: Dol – dolomite; Cal – calcite; Qz – quartz; Fsp – feldspar; Ilt/Ms – Illite/Muscovite; Chl – Chlorite; Mnt – montmorillonite; Kln – kaolinite.

Outcrop	Sample	Mineralogy
GCC	CER-1	Dol, Cal, Qz, Fsp, Ilt/Ms
	CER-2	Qz, Fsp, Cal, Dol, Ilt/Ms
Outcrop I	CER-3	Qz, Ilt/Ms, Fsp, Chl/Mnt, Cal
	CER-4	Qz, Ilt/Ms, Fsp, Chl/Mnt, Cal
Outcrop II	CER-5	Cal, Qz, Fsp, Ilt/Ms, Chl/Mnt
Outcrop III	CER-6	Qz, Ilt/Ms, Fsp, Chl/Mnt, Cal
	CER-7	Qz, Ilt/Ms, Fsp, Chl/Mnt, Cal
	CER-8	Qz, Ilt/Ms, Fsp, Chl/Mnt, Cal
	CER-9	Qz, Ilt/Ms, Fsp, Chl/Mnt
	CER-10	Qz, Ilt/Ms, Fsp, Chl/Mnt, Cal
	CER-11	Qz, Ilt/Ms, Fsp, Mnt, Cal
	CER-12	Qz, Ilt/Ms, Fsp, Chl/Mnt, Cal
	CER-13	Qz, Ilt/Ms, Fsp, Chl/Mnt
Outcrop IV	CER-14	Qz, Ilt/Ms, Fsp, Mnt, Kln

Turdaș Culture ceramics. Under OM the potsherds consist of a clayey matrix embedding larger aplastic phases (clasts). The matrix has an oriented texture, given by the arrangement of phyllosilicate minerals. Seen with crossed polarizers, the matrix is birefringent in most of the samples. Some samples show in places small isotropic parts. The aplastic clasts larger than 0.02 mm in size are predominantly muscovite and quartz. The lithoclasts are rare and include fragments of quartzite, micaschist, quartzo-feldspathic rock and carbonate rock. A fragment of a fossil bivalve was found in sample CE-261. Fe-rich pedogenic concretions occur as well. The size of the clasts varies from ~20 μm to ~2 mm (the largest ceramoclast), with an average of 45 μm. According to Wentworth (1922) scale, the average clasts plot within the coarse silt group. Most of the potsherds are predominantly semifine, only four sherds (CE-76, CE-260, CE-262, and CE-263) are coarse.

The diffractograms of the Turdaș sherds display a mineralogical composition with quartz, illite/muscovite, and feldspars as main mineral phases. The 10 Å, 4.5 Å and 2.6 Å illite/muscovite peaks are visible in all samples and show various intensities. There are no samples with missing muscovite/illite 10 Å peaks. The wide diffraction peak at 14 Å may be assigned to both chlorite and smectite (montmorillonite). A weak hematite peak (2.5 Å) occurs in few samples. The potsherds containing the 3.03 Å calcite peak have a highly birefringent matrix in OM.

The BSE images of the Turdaș potsherds illustrate an inhomogeneous ceramic body containing a high amount of phyllosilicate lamellae occurring as part of the matrix or as larger clasts. These lamellae are mainly muscovite. In the analyzed samples, the lithoclasts are represented by quartzites. Pedogenic concretions have been identified in sample CE-75. The matrix chemistry includes SiO_2 (between 47.51 and 50.32 mass%) and Al_2O_3 (between 16.06 and 35.12 mass%). The content of Al_2O_3 and SiO_2 is close to that of illite (Deer et al., 1992) which has 51.25 mass% SiO_2 and 23.53 mass% Al_2O_3. The amount of P_2O_5 is below 2 mass% and shows a positive correlation with CaO. Micas are represented by muscovite, which shows 0.79 to 3.55 mass% MgO and 0.44 to 5.64 mass% FeO_{TOT}. The pedogenic concretions contain ~35 mass% FeO_{TOT}, ~6 mass% Al_2O_3, ~4.2 mass% P_2O_5, ~5.4 mass% CaO and ~21 mass% SiO_2. K-feldspars contain between 13.2 and 16.3 mass% K_2O. Plagioclase show up to 12 mass% CaO ($An_{59.4}$ $Ab_{39.6}$ $Or_{1.1}$).

Foeni Group ceramics. Part of the results obtained by polarizing light optical microscopy, X-ray powder diffraction and electron microprobe analysis were previously published by Giurgiu et al. (2019). Under OM, the sherds show a random arrangement of phyllosilicate lamellae, except for samples CE-80, CE-81 and CE-83 which have a local oriented texture. Excepting the sample CE-79 which is semifine, all other sherds are fine-grained. With crossed polarizers, the matrix is birefringent in most of samples. The nonplastic clasts are mostly quartz, micas, plagioclase, alkali feldspars and heavy minerals, as well as lithoclasts and Fe-rich concretions. Quartz has angular and subangular shape and displays in some cases a network of cracks. Muscovite forms small or large lamellae, whereas biotite is either fresh, or partially altered to chlorite associated with opaque minerals. Polysynthetic-twinned plagioclase is frequent, whereas the alkali feldspar is rarer and slightly altered to fine-grained muscovite ("sericite"). Grains of epidote, clinozoisite staurolite, amphibole, garnet and apatite occur as well (Giurgiu et al., 2019). The lithoclasts are scarce and include quartzite, micaschist, amphibolitic schist and quartz-feldspar rock. Aggregates of opaque material, 25–50 μm in size, are iron pellets (so-called 'bohnerz' by Maggetti, 1979), Fe-rich pedogenic concretions and graphite lamellae. Clay pellets have also been identified. Ceramoclasts are found only occasionally, in the sherds CE-82 and CE-83. Granulometrically, only sample CE-79 is semifine; the remaining samples are finely-grained.

The diffractograms of Foeni sheds show a similar mineralogical composition for all sherds and indicate quartz, illite/muscovite, and feldspars as main mineral phases. The 10 Å peak is sharp and intense for the sherds with a highly birefringent matrix, which prove the crystalline structure of the illite/muscovite minerals. The wide diffraction peak at 14 Å may be assigned to both chlorite and smectite (montmorillonite). A weak hematite peak (2.5 Å) occurs in few samples. There are no diffractograms lacking the illite/muscovite peaks.

The back-scattered electron images and the energy-dispersive spectra for Foeni potsherds show a porous ceramic body, chemically and mineralogically inhomogeneous. The quartz fragments are prevalent, feldspars, muscovite and chlorite are common. Heavy minerals include apatite, epidote, clinozoisite, ilmenite and rarer amphibole. Ceramoclasts, chloritic schists, quartzo-feldspathic rock, soil concretions and clay pellets have also been identified. The values for SiO_2 range from 43.40 to 58.41 mass%, and Al_2O_3 from 18.59 to 29.30 mass%. The K_2O content shows a large variability, from 1.25 to 7.87 mass%. As for the Turdaș potsherds, the data

for the matrix in Foeni sherds, plotted in the K_2O-Na_2O-CaO ternary diagram, show a trend towards increasing CaO, in particular for the sample CE-83. The Al_2O_3 *vs.* SiO_2 diagram indicates an illite-like composition. With less than 3 mass% CaO, the matrix indicates a non-carbonatic clay as raw source for the ceramic paste. The P_2O_5 *vs* CaO diagram shows two matrix groups. The first group (A) includes a matrix with high calcium and increasing phosphorous contents and reveals a slightly positive correlation with the data obtained for a clay pellet and a ceramoclast. The second group (B) has low phosphorous and calcium contents. Micas are mostly muscovite and less chlorite. Muscovite shows 0.9 and 3.77 mass% MgO and 1.27 and 10.18 mass% FeO. The quartz grains are almost pure, with 99.14 mass% SiO_2. Data published by Giurgiu et al. (2019) indicate that the iron pellets/pedogenic concretions contain up to 20 mass% Fe_2O_3, ~13 mass% Al_2O_3, ~4.5 mass% P_2O_5, ~4.2 mass% CaO, ~35 mass% SiO_2 and ~10 mass% TiO_2. Alkali-feldspar shows an orthoclase composition, with less than 10% albite. Plagioclases do not display compositional zoning, are acidic to intermediate in composition and range from albite Ab_{92} to andesine $Ab_{67.9}$ (Giurgiu et al., 2019).

The secondary electron images reveal a porous and sintered ceramic body, which looks similar to the ceramic body obtained by Hein et al. (2008) when firing clays with 40% temper at temperatures in a wide range of temperatures, *i.e*. between 550 and 850 °C. The most important aspect is that which regards the surface treatment (finishing). Here we follow the description and grading of smoothing and burnishing provided by Ionescu et al. (2015, 2019) and Ionescu & Hoeck (2020). Two main styles of burnishing were identified: a linear (pattern) and a plain one, respectively. They occur on a generally smoothed surface, probably done with wet hand or a dump cloth (Ionescu & Hoeck, 2020). The features of the ceramic body beneath both types of burnish are similar. The burnished surfaces display a well-defined layer, 5 to 10 μm in thickness, consisting of a mass of compacted clay minerals, devoid of large clasts. Such a structure of a burnished surface was also described by Rutter (1975) and Ionescu et al. (2015). The surface of the burnished lines is marked by fine longitudinal striae. The plain burnished surface in sample CE-77 shows fine cracks and irregularities. Sample CE-82 displays burnished areas which are flat, even, and compact. Fine randomly oriented cracks interrupt the continuity of the burnishing. The movement direction of the tool during burnishing is indicated by the preserved fine striae.

Coțofeni Culture ceramics. Part of the polarizing light optical microscopy, X-ray powder diffraction and electron microprobe analysis results on Coțofeni ceramics have been published by Giurgiu et al. (2017b) and presented at various conferences (*e.g*. Giurgiu et al., 2016a, 2017a).

Unde OM the sherds show a clayey matrix, with various clasts embedded within it. Seen with one polarizer, the matrix appears as translucent to opaque, orange to dark brown mass. The texture is marked mostly by a random disposition of voids and phyllosilicate lamellae. Based on the optical characteristics of the matrix, the sherds were separated into three groups. The first group includes sherds with a highly birefringent matrix consisting of only slightly thermally transformed clay minerals. The second group shows an isotropic matrix. The third group of sherds contains a mixture of low birefringent and isotropic parts. The small bright red grains, irregularly distributed throughout the matrix, are either isotropic or slightly anisotropic.

The nonplastic clasts are mostly quartz, K-feldspar, muscovite, and rarer plagioclase. Quartz forms angular and sub-angular grains which are often highly fissured or have etched rims. Other minerals such as biotite, chloritized biotite, epidote group minerals (here referred as epidote), amphibole, staurolite, apatite, garnet, titanite, zircon and pyroxene were identified. The lithoclasts are mostly metamorphic rocks such as quartzite, muscovite-bearing quartzite, muscovite and biotite micaschist, gneiss, possibly graphitic schist, and amphibolite. Clasts of crystalline carbonate rocks are found in many sherds. Fragments of siderite and altered Fe-ore are present. The only igneous clasts include basalt and a granodiorite-type rock. The lithoclasts of sedimentary origin are sandstones.

Fragments of ceramoclasts are common and display different compositions and textures compared to the host. Additionally, soil concretions and small clay pellets were found. Also, samples CE-55 and CE-108 contain fossil remains, namely a ?gastropod and bryozoans, respectively.

The main XRPD peaks are given by illite/muscovite, quartz, and feldspars. The 2.69 Å hematite, the 3.03 Å calcite or the very weak 2.88 Å dolomite peaks are visible in few samples. The 14 Å peak can be assigned to both chlorite and montmorillonite. A 2.96 Å peak in CE-33 can be linked to clinopyroxene. A peak of talc (9.35 Å) is seen only in sample CE-31. The samples with a birefringent matrix display a sharp peak corresponding to still crystalline illite and muscovite. The samples with a mix of low birefringent and isotropic parts produced diminished illite/muscovite peaks due to the partial destruction of the crystalline structure. The

samples with an isotropic matrix do not have the 10 Å peak, but only a small lump between 20 and 45° 2θ – characteristic of an amorphous phase; other muscovite/illite peaks are still visible.

An inhomogeneous ceramic body is visible in the back-scattered electron images. The matrix contains variously-sized fragments of quartz, K-feldspar, muscovite, some plagioclase, chloritized biotite, and chlorite. Heavy minerals include rutile, apatite, epidote, monazite, ilmenite, titanite and zircon. The lithoclasts are quartzite, micaschist, gneiss, granodioritic rock and sandstone. All samples contain clay pellets and soil concretions as well as various types of ceramoclasts which usually show a contraction void around.

In the matrix, SiO_2 ranges from 45.02 to 55.32 mass%, K_2O from 1.51 to 5.33 mass% and FeO_{TOT} from 3.26 up to 14.07 mass%. CaO ranges between 0.92 and 2.32 mass%, with higher values, up to 6.5 mass%, being recorded only in sample CE-170. Sample CE-39 shows practically no CaO. P_2O_5 is generally below the detection limit, except in CE-170 where it ranges from 0.07 to 3.70 mass%.

The matrix is mainly composed of illite-like minerals. The K_2O *versus* Al_2O_3 diagrams display the wide chemical variation of the matrix. In some areas, tiny dark gray spots in the BSE image can be observed. There, the matrix has up to 60 mass% SiO_2. The matrix is characterized by a very low P_2O_5 content.

The clay pellets and the matrix have a similar chemistry, with Si, Al, and K as the main elements. They also contain low amounts of Mg, Fe, Ca, Ti, Na and even P. The soil concretions are dominated by Si, Al, and Fe, with some K, P, Mg and Ti.

The matrix of a few ceramoclasts has been analyzed as well. In the K_2O-Na_2O-CaO ternary diagram and in the Al_2O_3 *vs*. SiO_2 diagram our data plot close to illite. The K_2O *versus* Al_2O_3 diagram illustrates the chemical variation of the matrix of ceramoclasts. P_2O_5 correlates with CaO, excepting for a few analyzing points from a ceramoclast in samples CE-39 and CE-235 which practically contain no P_2O_5.

Micas are mostly muscovite, rarer being biotite and chloritized biotite. Muscovite occurs as large clastic lamellae, up to 300-400 μm in length, or as small relics, partly melted, in the matrix. Chemically, muscovite forms a homogeneous group, with Al_2O_3 and K_2O content in the normal range or slightly below. The significant amount of MgO and FeO, correlated with a surplus of SiO_2 in most of the muscovite proves its phengitic character.

Feldspars form either very small grains in the matrix or large crystals, up to 300 μm in size. All the K-feldspar are nearly pure in composition, with Na_2O content being mainly below 1 mass%, reaching up to 2 mass% in a few grains, resulting in 10 to 20 mol% albite respectively. No albite could be identified so far.

The SEM study focused on the surface treatment and decoration as well as the internal microstructure of the potsherds. Potsherd CE-58 shows an intensely fissured ceramic body embedding clasts with lamellar habitus. The surface of sample CE-58 is decorated with "U" shaped *incisions*. Very fine longitudinal striations present on the bottom of the channels offer a clue about the movement direction during the processes of incision. The remnants of burnished surfaces (compact, even and lacking distinguishable clasts) visible between incision lines proves that prior the decoration, the surface of the pot was carefully treated by burnishing. In the sample CE-91 the continuity of the burnished surface is interrupted by fine randomly oriented cracks or by some relief irregularities.

Discussions

Raw clays. The XRPD of whole ceramic body and the EPMA data on the matrix of Turdaș Culture, Foeni group and Coțofeni Culture sherds indicate essentially that an Fe-rich, illitic-like raw material was used to prepare the ceramic paste. The plot of data in the K_2O-Na_2O-CaO diagrams shows depletion in K_2O and enrichment in CaO compared to natural illite (Deer et al., 1992). The lower K_2O values are due the loss of K^+ following the start of dehydroxylation of illite-muscovite (Guggenheim et al., 1987; Rodriguez-Navarro et al., 2003; Gualtieri & Ferrari, 2006). The tendency to incorporate calcium into the illite-type structure was previously described by Ionescu & Hoeck (2011) in the matrix from some Copper Age ceramics from Romania. Apart of calcium related to illitic mass, the higher content of CaO in samples is due most likely to small amounts of montmorillonite (Giurgiu et al., 2019). A small amount of montmorillonite was identified in the Miocene geological samples taken from Peteac Valley which may have served as the source for the raw clays. The cave loam (CER-1 and CER-2) contains, as previously shown, a high amount of dolomite and calcite. This composition is not compatible with the composition of the potsherds from the three populations (Turdaș, Foeni and Coțofeni). It seems likely that the pots were produced far away from the areas where crystalline dolomite and calcite rocks occur. The crystalline carbonate rock fragments from the Coțofeni

potsherds may be interpreted as accidental and not intentionally added in the ceramic paste. Generally, it is considered that the P_2O_5 amount from pottery is due to finely grained apatite and pedogenic concretions present in the raw material (Ionescu et al., 2011) or is a product result of burial (Freestone et al., 1994; Maritan et al., 2009). In the matrix of *Turdaș* potsherds, the EMPA showed that P_2O_5 is below 2 mass% and has a positive correlation with CaO (0.98 correlation coefficient). This points to apatite as the source of P. The CaO vs. P_2O_5 diagram for the matrix of *Foeni Group* sherds displays two groups of data, one with higher calcium and phosphorous contents (A) and another with lower calcium and phosphorous contents (B). There is a positive correlation (~0.8) between P_2O_5 and CaO for group A which indicates apatite as the source of P for part of the matrix (see also Ionescu et al., 2011; Ionescu & Hoeck, 2017). On the other hand, phosphorous may be present as result of burial (Freestone et al., 1994; Maritan et al., 2009) in the case of the group B data (Giurgiu et al., 2019). In contrast with the Turdaș and Foeni sherds which contain phosphorous, the P_2O_3 amount for the matrix from Coțofeni sherds is very low (and frequently zero) indicating either a P-poor clay or no burial contamination.

Matrix EMPA data on ceramoclasts from a Foeni sample CE-83 (Foeni) plot in the same fields as the data from the host ceramic body. This result could point to the use of the same type of clay (*i.e.* illite-like) and the same clay source for producing the older vessels from which the analyzed ceramoclast originates. If the raw materials have a good quality, the continuity of exploiting the same source/outcrop is not surprising.

In the case of Coțofeni sherds, the matrix of ceramoclasts and the matrix of the ceramic body were compared. Overall, the values for the matrix from the ceramoclasts plot in the same fields as the values from the matrix of the ceramic body. Notable differences are present in the case of P_2O_5 which shows higher values in the ceramoclasts than in host ceramic body and it correlates with the CaO contents.

Tempering materials. For the sherd from all three population, the data support the existence of two types of temper: a natural one, *i.e*. a silty to sandy material (already present in the raw clayey material), and an artificial one, intentionally added by the potter in small amounts to better control the plasticity (Maggetti, 1979).

In Turdaș potsherds, the natural temper predominates. It consisted of a sandy/silty material with mainly quartz and muscovite. The semifine sherds display a relatively homogenous

ceramic body with a homogeneous distribution of the temper in the whole sherd, indicating a good mixing of the raw materials. Most of the samples contain mainly quartz and muscovite. It seems that the Turdaș potters used a narrow range of materials to prepare the paste for the semifine wares and they were restricted to clay mixed with some temper rich in quartz and muscovite.

Data from *Foeni* and *Coțofeni* ceramic indicate a mineralogical composition with quartz, feldspars, micas, some heavy minerals, and rock fragments (especially micaschists, quartzites, amphibolitic schist and quartzo-feldspathic rocks) for the silty sandy material used as temper. Soil concretions and clay pellets are common in the *Foeni* and *Coțofeni* sherds and probably they originate from the natural clay. Their presence suggests a poor homogenization of the paste (Medeghini & Nigro, 2017) or the use of unseasoned clays (Maritan, 2004). The artificial temper is represented by ceramoclasts. They are rarely found in the Foeni potsherds whereas in Coțofeni ceramic ceramoclasts show a large compositional variety and are very frequent.

Fossils. Fossils are good indicators in provenance studies (Quinn & Day, 2007; Fabbri et al., 2014). These were identified in *Turdaș* as well as in *Coțofeni* samples, but in very low number. A bivalve fragment was described from Turdaș sample CE- 261 and fossils from Coțofeni sherds are restricted to samples CE-55 and CE-108 (bryozoans and a ?gastropod, respectively).

The geological sample CER-5 (from outcrop II) contains large bivalve and gastropod fossils (possibly *Actaeonella sp.*). The outcrop II is located in the Peteac Valley, close to the outcrop III, where the geological samples (CER-6 to CER-13) which fit with the sherd composition have been sampled. The Upper Cretaceous deposits in the vicinity of Nandru locality contain bivalves and gastropods fossils (Forray, 1994). Also, a fauna rich in gastropods and bivalves is known from the Sarmatian deposits between Răcăștia and Nandru (Gheorghiu, 1954; Zágoršek et al., 2008) where rocks such as those from the Peteac Valley also occur. Bryozoans have been described from the Middle Miocene deposits close to Răcăștia where gastropods are common (Zágoršek et al., 2008).

In the case of Coțofeni population, another hint about the area explored when they looked for raw materials comes from the Cauce Cave, located close to the GCC. In the Coțofeni level of this cave an amulet made of a perforated *Conus fuscocingulatus* (Sztancs et al., 2005) was

exhumed. This fossil occurs at Buituri (Hunedoara) – a famous paleontological site, as well as at Popești locality, north from the Peteac Valley (Marincaș et al., 1969; Mureșan et al., 1980; Hladilová et al., 2004). This suggests that Coțofeni people might have known this clay source.

The scarcity of fossils in Turdaș and Coțofeni sherds could be explained through an intentional excluding of carbonate/fossils or by using clays with the composition similar to the ones described from outcrops I, II and III in Peteac Valley. It is highly probable that the potters produced the wares somewhere between Răcăștia, Buituri and Peteac Valley. All these facts point to a production place near the Cerna Valley area or towards the west where all the Miocene deposits have more or less the same composition. It is known that the potters preferred to use materials (clays as well as the temper) usually located at <10 km distance from the production center (Arnold, 1988) and the mentioned area meets this requirement. No sign or remnants of Turdaș, Foeni or Coțofeni firing devices or ceramic-related wastes have been found in the cave or in its vicinity. The wares were not produced there, but in a place with easy access to the raw materials, *i.e.* silty mudstones, alluvial sands, and silts (Giurgiu et al., 2017b). The wares were most likely transported to the cave, which was only a temporary settlement usually used by the shepherds.

Firing conditions. The main clue to the firing atmosphere is the color and its variation within the wall of the pot. The ceramic wall of most Turdaș samples is homogenous, and indicates firing under constant redox conditions (Shepard 1956; Murad & Wagner 1996; Molera et al. 1998). Same conditions are inferred for few Foeni sherds which are homogenous in fresh crosscut. The Foeni sherds displaying reddish brown colors contain hematite and were fired in an oxidizing atmosphere. Most of the Coțofeni sherds display dark brownish and dark grayish colors, indicating a Fe-rich paste fired mostly in reducing conditions (Shepard, 1956; Kreimeyer, 1987; Murad & Wagner 1996; Molera et al., 1998). Still, the orange color for some samples and the presence of hematite suggest that some oxygen was still present in the kiln.

The bizonal structure of Turdaș sample CE-260 with red core and gray rims indicates a variable firing atmosphere: oxidizing at the beginning and reducing towards the end of the firing. The Coțofeni wares with color zoning *i.e*. bi-zonal and sandwich-type, were probably fired in a variable atmosphere (Molera et al., 1998; Nodari et al., 2007).

Foeni samples CE-79, CE-80 and CE-81 display a black-topped chromatic effect at the surface of the sherd and were intentionally fired to obtain this aesthetically aspect. The firing experiments carried out either in open air or in kilns show that the black-topped ceramics is produced by arranging the pots bottom-up on a floor covered by chaff, sawdust, oak wood or a mix of carbon and ash (Hendrickx et al., 2000; Baba & Saito, 2004; Bințințan, 2013; Bințințan & Gligor, 2016). In order to obtain such pots, a firing temperature below 900º-950º C is required (Dufournier, 1986).

The thermal conditions for the pottery are best reflected by the OM, EMPA and XRPD data. The optical characteristics of the matrix reflect the changes in the clay minerals' crystalline structure upon firing (Maggetti, 1982). The XRPD illite/muscovite peaks are good indicators of the changes suffered by the crystalline structure of the clay minerals during firing (Mercader et al., 2000; Broekmans et al., 2004; Ionescu et al., 2007).

The ceramic body of Turdaș sherds shows a highly birefringent matrix (Giurgiu et al., 2016b). Limited areas with low birefringence matrix are present in few sherds demonstrating advanced destruction of the phyllosilicates. No glass is present because the firing temperatures were not high enough to yield such a product. In the BSE images, muscovite appears as lamellae with fine cleavage lines, proving a low temperature of firing. Also, the carbonate is a good indicator of the firing temperature. The bivalve shell shows birefringence and indicates slight change during the ceramic firing, which can be estimated below 800 °C (see *e.g.*, Fabbri et al., 2014). At ~850 °C, calcite would start to decompose and form wollastonite, gehlenite or/and clinopyroxene (Rodriguez-Navarro et al., 2009).

Similarly, the OM study of Foeni sherds shows that most of the potsherds have a highly birefringent matrix composed of phyllosilicates sintered together. Still, the individual lamellae can be recognized and the crystal structure of the clay minerals is not significantly affected by temperature. There is no glass demonstrating that the temperature was not high enough to melt the material (Giurgiu et al., 2019).

It is known that illite-muscovite XRPD peaks are still present in the material fired at 800°C (Mercader et al., 2000) and that the destruction of illite begins at 820°C (Heimann, 2017). There are no Turdaș and Foeni diffractograms with missing illite/muscovite peaks, thus pointing to temperatures below 900 °C for all samples. The illite-muscovite diffraction peaks for most of the Turdaș and Foeni samples are very intense and sharp and a firing temperature of about 800

°C can be assigned to these sherds (see *e.g.*, Mercader et al., 2000). Samples (*e.g.* CE-69, CE-72, CE-75, and CE-262 from Turdaș, and CE-77 and CE-79 for Foeni) which show significant diminishing of the illite-muscovite diffraction peaks due to the partial destruction of the crystalline structure, argue for a firing temperature around 850 °C (Broekmans et al., 2004; Ionescu et al., 2007). These values are within the normal interval recorded in bonfires and surface clamps (Velde & Druc, 1999) and are high enough to produce a sintered ceramic body.

Muscovite dehydroxylation takes place in a large interval, between 700 and 1000 ºC (Mazzucato et al., 1999), whereas that of illite starts at 875 ºC and lasts until 1070 ºC (Gualtieri & Ferrari, 2006). The lower K_2O values obtained by EMPA for the Turdaș, Foeni and Coțofeni matrix are due the loss of K^+ following the start of dehydroxylation of illite and muscovite (Guggenheim et al., 1987; Rodriguez-Navarro et al., 2003; Gualtieri & Ferrari, 2006). These reactions suggest a firing temperature which might have reached 850 ºC in Turdaș ceramics, but only for a short period of time. The increasing CaO content can be explained through its incorporation upon firing at approximately 850°C (Ionescu & Hoeck, 2011).

In the case of Coțofeni ceramic the results point to three groups as regards the firing temperature: a low-fired, a medium-fired, and a high-fired group, respectively. However, there is a continuous transition between the groups and no sharp boundaries (Giurgiu et al., 2017b).

The low-fired Coțofeni sherds are easily identified after the highly birefringent matrix and untransformed carbonate clasts (*e.g.* CE-183). In samples CE-170 and CE-235, the clay minerals composing the matrix are sintered together. Individual lamellae are still present. These samples also have the most intense illite/muscovite XRPD peaks. All these features suggest a ~800 °C firing temperature (see also Meldau & Robertson, 1953; Cultrone et al., 2001; Grifa et al., 2009; Trindade et al., 2009; Maggetti et al., 2011; Rat'ko et al., 2011). The highly-fired sherds display a homogeneous matrix which has round pores. The birefringence is low and sometimes isotropic areas are present, proving the destruction of the crystalline structure of the clay minerals. Some of the carbonate clasts from these samples are partly thermally transformed (coronitic structure?). Some sherds do not show the 10 Å illite/muscovite diffraction peaks. Overall, these features indicate a ~900 °C firing temperature (Murad & Wagner 1998; Cultrone et al., 2001; Bertolino & Fabra, 2003; Trindade et al., 2009). The absence of an extensive vitrification demonstrates that the temperature was below 950 °C. The medium-fired sherds display a matrix consisting of low birefringent parts mixed with isotropic parts (*e.g.* CE-3). Some

quartz grains have etched margins and micas show signs of melting. The illite/muscovite diffraction peaks are diminished but not absent (*e.g.*, CE-1 and CE-31). These transformations indicate firing at temperatures reaching ~850 °C (Giurgiu et al., 2017b).

Firing devices. The lack of firing device near the cave or in the places where the raw materials are at hand suggests that temporary firing structures may have been used by Turdaș, Foeni and Coțofeni potters. The sherds were fired in surface clamps or bonfires which consisted of a pit where the pots were arranged and covered with fuel and subsequently fired. However, the identification of these firing devices is difficult and if they were used only seasonally, the reconstruction was more advantageous (Thér, 2004). The temperature values are within the normal interval recorded in bonfires and surface clamps (Velde & Druc, 1999) and are high enough to produce a sintered ceramic body. Data from Livingstone Smith (2001) shows that firing temperatures in bonfires and pits are usually around 800-850 ºC, but may reach >900 ºC, which is consistent with the inferred temperatures for the potsherds from all three populations.

The lack of firing device remnants and the successful experimental production of black topped ceramics not only in bicameral vertical kilns, but also in open-air (Hendrickx et al., 2000; Baba & Saito, 2004; Bințințan, 2013; Bințințan & Gligor, 2016) argue for the use of temporary firing structures by the Foeni potters.

The large thermal interval which was inferred for the Coțofeni ceramics may be due to the firing conditions, carried out in surface clumps or primitive ovens. Temperature homogeneity in clamps and kilns is difficult to acquire (Thér, 2014). The lowest temperature difference between two thermocouples obtained by Thér (2004) was in a two-chamber vertical kiln with grate and was of 40 °C. The same author has measured a difference of 248 ºC in clamp-kilns during one firing and highlighted that the temperature development is highly unstable in this type of kilns. Additionally, the thermal variation in a pot is normal and differences such as 390 ºC may occur between one part of the ceramic wall and another during one firing (Magetti et al., 2011). Consequently, it is highly plausible that low-, medium- and high-fired sherds could have been part of the same batch and fired together.

Decoration. Six Turdaș potsherds show plain burnish decoration on the exterior of the pot or on both sides, inner and outer. Also, burnish decoration is known as one of the characteristics

of Foeni Group pottery (Gligor, 2008) which shows not only plain burnished wares, but also pattern burnished surfaces.

The characteristic movement for producing burnished surfaces is rubbing back and forth the surface of the pot with a tool such as water-worn pebbles, lithic pestles, flint, or agate (Ionescu et al., 2015; Ionescu & Hoeck, 2020). Burnishing produces a thin film of well-aligned phyllosilicates, parallel to the surface, sealing off the holes and significantly diminishing the roughness (Ionescu et al., 2015, 2019; Ionescu & Hoeck, 2020). The resulted aspect obtained by the burnishing is a lustrous, shiny surface.

The SEM study of the Foeni ceramic show that small ridges separate the burnished pattern lines by the rest of the surface. By pressing the burnishing tool against the pot surface, the resulting burnished depressions display a slightly curved profile. These features point out to the use of a tool with rounded form. A water-worn pebble might have been the tool for making the burnished lines as they are highly available in the areas where the raw materials occur.

For Coțofeni samples, the surfaces are decorated with burnished surfaces located in between "U" shaped incisions. The latter are defined as a freehand decoration performed through pressing or cutting lines into the paste (Shepard, 1956). The combination of incisions and burnish decoration allows the identification of the order in which the pots were decorated. Usually, the pottery was incised after being burnished. This is also the case for sample CE-58 which is sharp and shows no overhang at the edges of incisions (Shepard, 1956). The incision was probably performed when the paste was plastic using a pointed tool held as a pencil and had a rounded point, producing the symmetrical and curved incision from sample CE-58. A similar process was probably implemented to the rest of the incised potsherds, as the majority shows the same characteristics as sample CE-58.

GENERAL CONCLUSIONS

The ^{14}C ages obtained from the Great Cave of Cerișor and the Cauce Cave are in stratigraphic order, with the oldest date indicating a Late Neolithic level in the profiles from both caves. From the Great Cave of Cerișor, the dated charcoal samples returned the following ages: 5,740 ± 40 B.P. (Late Neolithic, Turdaș Culture), 4,370 ± 35 B.P. (Copper Age, Coțofeni

Culture) and 3,490 ± 35 B.P. (Bronze Age, Wietenberg Culture). For the Cauce Cave the obtained ^{14}C dates are 5,880 ± 35 B.P. and 5,867 ± 34 B.P. (Late Neolithic, Turdaș Culture), 5,034 ± 30 B.P. (Copper Age, Hunyadihálom Culture) and 3,626 ± 30 B.P. (Bronze Age, Wietenberg Culture). The results correlate well with the inferred cultures/groups previously established by archaeologists for these caves. The ^{14}C data also comply with other absolute ages from literature. The past hydroclimate information was established based on $\delta^{13}C$ measured on archaeological charcoal. The paleohydroclimate during the Late Neolithic–Bronze Age interval was characterized by two dry episodes at ~5,500 cal B.P. and at ~4,200 cal B.P. and correlates with data from other paleoclimate archives. At 4.2 ka the Meghalayan stage begun and is clearly marked in the records from Great Cave of Cerișor and Cauce Cave. The approach is new in Romania and is suitable from other archaeological sites where charcoal is abundant.

Regarding the ceramics, the *Turdaș* potters produced semifine and coarse wares decorated with plain burnish. The population preferred reddish hues for the wares and firing took place in an oxidizing atmosphere. *Foeni* population, despite the primitive firing conditions in bonfires or surface clamps and the relatively low temperature attained, succeeded to produce blacked-topped ceramics, showing care for the aesthetical aspects and a certain control of the atmosphere in the kiln. Also, the potters were experienced in burnishing the wares, producing pattern and plain burnished ceramics for a better aspect, but also because they were probably aware of the better resistance of burnished pots. The *Coțofeni* potsherds form a homogeneous group, having the same composition and technological characteristics. The sherds are decorated with various motifs using techniques such as burnishing, incision and impression performed with pebbles, bones, and/or specialized wooden sticks. The raw clays were Fe-rich, illitic and K-poor. Most *Turdaș* potsherds have a temper consisting of a sandy material naturally occurring in the clays or intentionally added. *Foeni* potters occasionally added ceramoclasts for a better plasticity, but the temper was mainly natural, represented by a sandy material. For *Coțofeni*, the ceramic body is coarse and contains a high amount of temper represented by sand originating from a metamorphic hinterland. In contrast with Turdaș and Foeni, the ceramoclasts are ubiquitous which demonstrates that reusing older ceramic wares was common. The matrix of ceramoclasts show a composition almost identical with that of the matrix from the host ceramic body, pointing to the continuity in using the same raw clay source for longer periods of time.

The inferred temperature for *Turdaș* wares is below 850 °C, for *Foeni* ceramics is around 850 °C, and for *Coțofeni* sherds is between ~800 and ~900 °C. The large inhomogeneous distribution of temperature in the primitive firing devices and inside the ceramic wall is most likely responsible for the existence of this variation.

Considering the composition of the sherds from all three populations (with scarce crystalline carbonates), the production center was not located at the cave, but in a place where the raw materials were at hand. Also, the inferred raw materials point to a continuity in using the same raw materials source. Regarding the production place, as no remains of pits or other firing devices are known, the firing must have taken place in temporary surface clamps or bonfires which were rebuilt seasonally.

SELECTED REFERENCES

Aguilera M., Espinar C., Ferrio J.P., Pérez G., Voltas J. (2009): A map of autumn precipitation for the third millennium BP in the Eastern Iberian Peninsula from charcoal carbon isotopes. *Journal of Geochemical Exploration*, **102**, 157–165.

Aguilera M., Ferrio J.P., Pérez G., Araus J.L., Voltas J. (2012): Holocene changes in precipitation seasonality in the western Mediterranean Basin: a multi-species approach using $\delta^{13}C$ of archaeobotanical remains. *Journal of Quaternary Science*, **27** (2), 192–202.

Arnold D.E. (1988): Ceramic theory and cultural processes. Cambridge University Press, 279 p.

Audiard B., Thery-Parisot I., Blasco T., Mologni C., Texier P.-J., Battipaglia G. (2019): Crossing taxonomic and isotopic approaches in charcoal analyses to reveal past climates. New perspectives in Paleobotany from the Paleolithic Neanderthal dwelling-site of La Combette (Vaucluse, France). *Review of Palaeobotany and Palynology*, **266**, 52–60.

Baba M., Saito M. (2004): Experimental studies on the firing methods of black topped pottery in Predynastic Egypt. In: *Egypt at its origins: Studies in memory of Barbara Adams: Proceedings of the International Conference, 'Origin of the state: Predynastic and Early Dynastic Egypt', Kraków, 28th August–1st September 2002* (S. Hendrickx, R.F. Friedman, K.M. Ciałowicz, M. Chłodnicki, editors), pp. 575–589. Orientalia Lovaniensia Analecta 138, Peeters Publishing Leuven.

Balintoni I. (1997): Geotectonics of the metamorphic terrains from Romania. Ed. Carpatica, Cluj-Napoca, 176 pp. (in Romanian).

Balintoni I., Balica C., Ducea M.N., Stremțan C. (2011): Peri-Amazonian, Avalonian-type and Ganderian-type terranes in the South Carpathians, Romania: The Danubian domain basement. *Gondwana Research*, **19**, 945–957.

Baton F., Nguyen Tu T.T., Derenne S., Delorme A., Delarue F., Dufraisse, A. (2017): Tree-ring $\delta^{13}C$ of archeological charcoals as indicator of past climatic seasonality. A case study from

the Neolithic settlements of Lake Chalain (Jura, France). *Quaternary International*, **457**, 50–59.

Bălan G., Quinn C.P., Hodgins G. (2016): The Wietenberg culture: periodization and chronology. *Dacia N.S.*, LX, 67-92.

Berden G., Engeln R. (2009): Cavity Ring-down Spectroscopy: Techniques and Applications. Wiley, p. 344.

Bertolino S.R., Fabra M. (2003): Provenance and ceramic technology of pot sherds from ancient Andean cultures at the Ambato valley, Argentina. *Applied Clay Science*, **24**, 21–34.

Bințințan A. (2013): Arheologie experimentală. Arderea controlată în aer liber – o posibilă modalitate de obținere a efectului cromatic black-topped. *Buletinul Cercurilor Ştiinţifice Studenţeşti*, **19**, 7–19.

Bințințan A., Gligor M. (2016): Pottery kiln: A technological approach to Early Eneolithic black-topped production in Transylvania. *Studia Antiqua et Archaeologica*, **22**(1): 5–18.

Bird M.I., Ascough P.L. (2012): Isotopes in pyrogenic carbon: A review. *Organic Geochemistry*, **42** (12), 1529–1539.

Bojadžiev J. (1998): Radiocarbon dating from Southeastern Europe. In *James Harvey Gaul. In Memoriam* (Stefanovich M., Todorova H., Hauptmann H., eds.), vol. I, The James Harvey Gaul Foundation, Sofia, pp. 349-370.

Boroffka N. (1995) Cultura Wietenberg/The Wietenberg Culture. In Comori ale epocii bronzului din România/Treasures of the Bronze Age in Romania (Stoica C., Rotea M., Boroffka N., eds.), București, pp. 274-276 (in Romanian)/pp. 280–281 (in English).

Boroffka N. (2013) Romania, Moldova and Bulgaria. In: *The Oxford handbook of the European Bronze Age* (Harding A., ed.), Fokkens H. Oxford University Press, pp. 877–897.

Boroneanț V. (2000): The archaeology of caves and mines from Romania (in Romanian). cIMeC, București, 325 p.

Bräutigam A., Schlüter U., Eisenhut M., Gowik U. (2017): On the Evolutionary Origin of CAM Photosynthesis. *Plant Physiology*, **174** (2), 473–477.

Broekmans T., Adriaens A. & Pantos E. (2004): Analytical investigations of cooking pottery from Tell Beydar (NE-Syria). *Nuclear Instruments and Methods in Physics Research B: Beam Interactions with Materials and Atoms*, **226**, 92–97.

Bronk Ramsey C. (2017): Methods for Summarizing Radiocarbon Datasets. *Radiocarbon*, **59**(6), 1809–1833.

Bronk Ramsey C., Lee S. (2013): Recent and planned developments of the program OxCal. *Radiocarbon*, **55**(2-3), 720–730.

Brugnoli E., Farquhar G.D., (2000): Photosynthetic fractionation of farbon isotopes. In *Photosynthesis: Physiology and Metabolism* (R.C. Leegood, T.D. Sharkey, S. von Caemmerer eds), Kluwer Academic Publishers, Dordrecht, pp. 399–434.

Brummack S. (2015): New Radiocarbon Dates from Eastern Slovakia The Cases of Malé Raškovce and Barca Baloty. In *Neolithic and Copper Age between the Carpathians and the Aegean Sea: Chronologies and Technologies from the 6th to the 4th Millennium BCE: International Workshop Budapest 2012 (Volume 31 of Archäologie in Eurasien*) (Hansen S., Raczky P., Anders A., Reingruber A., eds.). Habelt Verlag, Bonn, pp. 1–19.

Brummack S., Diaconescu D. (2015): A Bayesian Approach of the AMS data from the Great Hungarian Plain's Copper Age (in Romanian). Analele Banatului, S.N., Arheologie – Istorie, XXIII, 101–118.

Busch K.W., Busch M.A. (1999): Cavity-ringdown Spectroscopy: an Ultratraceabsorption Measurement Technique. American Chemical Society, Washington, p. 269.

Campbell J.W., Waters M.N., Rich F. (2017): Guano core evidence of palaeoenvironmental change and Woodland Indian inhabitance in Fern Cave, Alabama, USA, from the mid-Holocene to present. *Boreas*, **46** (3): 462–469.

Cerling T.E., Harris J.M., MacFadden B.J., Leakey M.G., Quade J., Eisenmann V., Ehieringer J.R. (1997): Global vegetation change through the Miocene/Pliocene boundary. *Nature*, **389**, 153–158.

Chirică N., Rănceanu V. (1976): Sub cerul purpuriu al Hunedoarei. Hunedoara, 224 p.

Ciugudean H. (2000): The Late Eneolithic in Transilvania and Banat: the Coţofeni culture. Ed. Mirton, Bibliotheca Historica et Archaeologica Banatica Timişoara, 124 pp.

Cleary D.M., Feurdean A., Tanțău I., Forray F.L. (2019): Pollen, $\delta^{15}N$ and $\delta^{13}C$ guano-derived record of late Holocene vegetation and climate in the southern Carpathians, Romania. *Review of Palaeobotany and Palynology*, **265**, 62–75.

Cohen-Ofri I., Weiner L., Boaretto E., Mintz G., Weiner S. (2006): Modern and fossil charcoal: aspects of structure and diagenesis. *Journal of Archaeological Science*, **33**, 428–439.

Constantin, S., Bojar, A.-V., Lauritzen, S.-E., Lundberg, J. (2007): Holocene and Late Pleistocene climate in the sub-Mediterranean continental environment: A speleothem record from Poleva Cave (Southern Carpathians, Romania). *Palaeogeography, Palaeoclimatology, Palaeoecology*, **243**, 322–338.

Coplen, T.B., 2011. Guidelines and recommended terms for expression of stable isotope-ratio and gas-ratio measurement results. *Rapid Communications in Mass Spectrometry*, **25**, 2538–2560.

Cultrone G., Rodriguez-Navarro C., Sebastian E., Cazalla O., De la Torre M.J. (2001): Carbonate and silicate phase reactions during ceramic firing. European Journal of Mineralogy, **13**, 621–634.

Deer W.A., Howie R.A., Zussman J. (1992): An Introduction to the Rock-Forming Minerals, 2nd edn. Pearson Prentice Hall, London, UK, 696 pp.

Diaconescu D. (2014): About Turdaș Culture and its chronological position. *Analele Banatului, S.N., Arheologie-Istorie*, XXII, 69–90 (in Romanian).

Diaconescu D., Tincu S. (2016): Consideraţiii arherologice privind necropola tumulară de la Silvaşu de Jos – „Dealu Țapului" (oraş Haţeg, jud. Hunedoara). *Analele Banatului, S.N., Arheologie – Istorie*, XXIV, 107–141.

Dibble H.L., Berna F., Goldberg P., McPherron S.P., Mentzer S., Niven L., Richter D., Sandgathe D., Théry-Parisot I., Turq A. (2009): A Preliminary Report on Pech de l'Azé IV, Layer 8 (Middle Paleolithic, France). *PaleoAnthropology*, 2009, 182–219.

Drașovean F. (2013): About some synchronisms from the late Neolithic and Early Eneolithic in Banat and Transilvania. A Bayesian approach of some absolute data previously published. *Analele Banatului, Arheologie – Istorie*, XXI, 11–34 (in Romanian).

Drașovean F. (2004): Transylvania and the Banat in the Late Neolithic. The origins of the Petrești Culture. *Antaeus*, 27, 27–36

Dufournier D. (1986): Analyse de la céramique, premiers résultants. In: *Saï 1 La nécropole Kerma* (B. Gratien, ed.), Éditions du CNRS, Paris, France, pp. 444–446.

Enea-Giurgiu A., Ionescu C., Hoeck V., Tămaș T., Roman C. (2018): Eneolithic pottery from Southern Carpathians (Romania): An archaeometric study. XXI International Congress of the Carpathian Balkan Geological Association (CBGA), September 10–13, 2018, Salzburg

(Austria). *Geologica Balcanica, Abstracts* (Neubauer F., Brendel U., Friedl G., eds.), p. 371.

Enea-Giurgiu A., Ionescu C., Hoeck V., Tămaş T., Roman C. (2019): Overview of the ceramic technology from Late Neolithic to Copper Age in the Southern Carpathians, Romania. Presented at the 16th European Meeting on Ancient Ceramics, Barcelona. *Conference programme and abstracts*, p. 176.

Fabbri B., Gualtieri S., Shoval S. (2014): The presence of calcite in archeological ceramics. *Journal of the European Ceramic Society*, **34**, 1899–1911.

Farquhar G.D., Ehleringer J.R., Hubick K.T. (1989): Carbon isotope discrimination and photosynthesis. *Annual Review of Plant Physiology and Plant Molecular Biology*, **40**, 503-37.

Farquhar G.D., Schulze E.-D., Kuppers M. (1980): Responses to humidity by stomata of Nicotiana glauca L. and Corylus avellana L. are consistent with the optimization of carbon dioxide uptake with respect to water loss. *Australian Journal of Plant Physiology*, **7**, 315–327.

Ferrio J.P., Alosno N., Lopez J.B., Araus J.L., Voltas J. (2006): Carbon isotope composition of fossil charcoal reveals aridity changes in the NW Mediterranean Basin. *Global Change Biology*, **12 (**7), 1253–1266.

Feurdean A., Vasiliev I. (2019): The contribution of fire to the late Miocene spread of grasslands in eastern Eurasia (Black Sea region). *Scientific Reports*, **9**, Article number 6750.

Filipaş L., Bărbos M., Coldea Gh. (2013): A new syntaxon of fir forests (Abies alba) from South-Eastern Carpathians (Romania). *Contribuţii Botanice*, **XLVIII**, 69–73.

Florescu G., Brown K.J., Carter V.A., Kuneš P., Veski S., Feurdean A. (2019): Holocene rapid climate changes and ice-rafting debris events reflected in high-resolution European charcoal records. *Quaternary Science Reviews*, **222**, 105877.

Forenbaher S. (1993) Radiocarbon dates and absolute chronology of the Central European Early Bronze Age. *Antiquity*, **67**, 218–256.

Forray F. (1994): Formațiuni mezozoice din regiunea Nandru-Cherghеș, Cluj-Napoca. Dipoloma thesis, unpublished (in Romanian). Babes-Bolyai University Cluj-Napoca.

Forray F.L., Onac B.P., Tanțău I., Wynn J.G., Tămaș T., Coroiu I., Giurgiu A.M. (2015): A Late Holocene environmental history of a bat guano deposit from Romania: an isotopic, pollen and microcharcoal study. *Quaternary Science Reviews*, **127**, 141–154.

Freestone I.C., Middleton A.P., Meeks N.D. (1994): Significance of phosphate in ceramic bodies: discussion of paper by Bollong et al., *Journal of Archaeological Science*, **2**1, 425–426.

Hladilová Š., Zágoršek K., Ziegler V. (2004): Middle Miocene gastropod shell with epifauna from the locality Buituri (Transylvanian Basin, Romania). *Fragmenta Palaeontologica Hungarica*, **22**, 99–105.

Gheorghiu C. (1954): Geological study of the Mureşului Valley between Deva and Dobra. *Anuarul Comitetului Geologic*, **27,** 78-174.

Giurgiu, A., Ionescu, C., Hoeck, V. (2016a): Grog-tempered Copper Age pottery in Southern Carpathians (Romania): technological choice or just a happening? Book of Abstracts, 8-Mid European Clay Conference, 4-8 July 2016, Košice, Slovakia, p. 189, ISBN 978-80-972288-0-4.

Giurgiu A., Ionescu C., Hoeck V., Tămaș T., Roman C. (2016b): Technological constraints for Late Neolithic pottery found in the Southern Carpathians (Romania). Book of abstracts, *2nd European Mineralogical Conference, 11-15 September 2016, Rimini, Italy*, p. 709.

Giurgiu A., Ionescu C., Tămaş T., Hoeck V., Roman C. (2017a): Copper Age ceramics from the Cerișor Cave (Southern Carpathians, Romania). *Proceedings of the 17th International Congress of Speleology, vol. 1 (Ed. 2) (K. Moore, S. White, eds.)*, p. 15, ISBN 978-0-9588857-0-6.

Giurgiu A., Ionescu C., Hoeck V., Tămaș T., Roman C., Crandell O. (2017b): Insights into the raw materials and technology used to produce Copper Age ceramics in the Southern Carpathians (Romania). *Archaeological and Anthropological Sciences*, **9** (6), 1259–1273.

Giurgiu A., Ionescu C., Hoeck V., Tămaș T., Roman C. (2019): An archaeometric study of early Copper Age pottery from a cave in Romania. *Clay Minerals*, **54** (3), 255–268.

Gligor M. (2008): Contributions to the repertory of the discovenes belonging to Foeni group of Romania. *Patrimonium Apulense*, **VII-VIII**, 11–18.

Gligor M. (2009): The Neolithic and Eneolithic settlement from Alba Iulia – Lumea Nouă in the focus of recent research. *Ed. Mega, Cluj-Napoca*, 487 pp. (in Romanian).

Gligor M. (2014): The beginnings of the Early Eneolithic in Transylvania: a Bayesian approach. *Analele Banatului*, **XXII**, 91–105 (in Romanian).

Grapes R. (2011): Pyrometamorphism, 2nd edn. *Springer, Berlin-Heidelberg*, 365 p.

Grifa C., Cultrone G., Langella A., Mercurio M., De Bonis A., Sebastián E., Morra V. (2009): Ceramic replicas of archaeological artefacts in Benevento area (Italy): petrophysical changes induced by different proportions of clays and temper. *Applied Clay Science*, **46**, 231–240.

Grootes P.M, Stuiver M. (1997): Oxygen 18/16 variability in Greenland snow and ice with 10-3 to 10-5-year time resolution. *Journal of Geophysical Research: Oceans*, **102**(C12), 26455-26470.

Gualtieri A.F., Ferrari S. (2006): Kinetics of illite dehydroxylation. *Physics and Chemistry of Minerals*, **33**, 490–501.

Guggenheim S., Chang Y.H., van Gross K.A.F. (1987): Muscovite dehydroxylation: high-temperature studies. *American Mineralogist*, **72**, 537–550.

Hall G., Woodborne S., Scholes M. (2008): Stable carbon isotope ratios from archaeological charcoal as palaeoenvironmental indicators. *Chemical Geology*, **247**, 384–400.

Heimann R. (2017): X-Ray Powder Diffraction (XRPD). In: *The Oxford Handbook of Archaeological Ceramic Analysis (Hunt A. ed.)*, Oxford University Press, Oxford, UK, pp. 327–341.

Hendrickx S., Friedman R., Loyens F. (2000): Experimental archaeology concerning black-topped pottery from Ancient Egypt and the Sudan. *Cahiers de le Céramique Egyptienne*, **6**, 171–187.

Hunt A.M. (2017): Introduction to the Oxford Handbook of Archaeological Ceramic Analysis. In: *The Oxford Handbook of Archaeological Ceramic Analysis* (Hunt. A, ed), Oxford University Press, Oxford, UK, pp. 3-6.

Iancu V., Berza T., Seghedi A., Gheuca I., Hann H.P. (2005a): Alpine polyphase tectono-metamorphic evolution of the South Carpathians: A new overview. *Tectonophysics*, **410**, 337–365.

Iancu V., Berza T., Seghedi A., Mărunțiu M. (2005b): Palaeozoic rock assemblages incorporated in the South Carpathian alpine thrust belt (Romania and Serbia): A review. *Geologica Belgica*, **8** (4), 48–68.

Ionescu C., Ghergari L. (2007): Caracteristici mineralogice si petrografice ale ceramicii romane din Napoca. In *Ceramica romană din Napoca* (V. Rusu-Bolindeț, ed.). Editura Mega Cluj-Napoca, *Biblioteca Mvsei Napocensis*, **XXV**, 434–462.

Ionescu C., Fischer C., Hoeck V., Lüttge A. (2019): Discrimination of ceramic surface finishing by vertical scanning interferometry. *Archaeometry*, **61 (**1), 31–42.

Ionescu C., Hoeck V. (2011): Firing-induced transformations in Copper Age ceramics from NE Romania. *European Journal of Mineralogy*, **23**(6), 937–958.

Ionescu C., Hoeck V. (2017): Electron Microprobe Analysis (EMPA). In: *The Oxford Handbook of Archaeological Ceramic Analysis* (Hunt A., ed.), Oxford University Press, pp. 288–304.

Ionescu C., Hoeck V. (2020): Ceramic technology. How to investigate ceramic surface finishing. In Gliozzo E. (ed), Ceramics: Research questions and answers. *Archaeological and Antrhopological Sciences* https://doi.org/10.1007/s12520-020-01144-9.

Ionescu C., Hoeck V., Crandell O.N., Šaric K. (2015): Burnishing versus smoothing in ceramic surface finishing: A SEM study. *Archaeometry,* **57** (1), 18–26.

Ionescu C., Hoeck V., Ghergari L. (2011): Electron microprobe analysis of ancient ceramics: A case study from Romania. *Applied Clay Science,* **53** (3), 466–475.

Kacsó C (2004): Mărturii arheologice, Ed. Nereamia Napocae, Baia Mare, 211 p.

Kacsó C. (2015): Repertoriul arheologic al județului Maramureș, Volumul I, 2nd ed., Ed. Ethnologica, 653 p.

Kanthilatha N. (2016): Sediments as artefacts: geoarchaeological study of prehistoric sediments in Northwest Thailand. *PhD Thesis*, Southern Cross University, Lismore, NSW, 325 p.

Karkanas P., Goldberg P. (2019): Reconstructing archaeological sites. Understanding the geoarchaeological matrix. John Wiley & Sons, 279 p.

Kohn M.J. (2010): Carbon isotope compositions of terrestrial C3 plants as indicators of (paleo)ecology and (paleo)climate. *Proceedings of the National Academy of Sciences*, **107**, no. 46, 19691-19695.

Kohn M.J. (2016): Carbon isotope discrimination in C3 land plants is independent of natural variations in pCO2. *Geochemical Perspectives Letters*, **2**, 35-43.

Krull E.S., Skjemstad J.O., Graetz D., Grice K., Dunning W., Cook G., Parr J. F. (2003): ^{13}C-depleted charcoal from C_4 grasses and the role of occluded carbon in phytoliths. *Organic Geochemistry*, **34 (**9), 1337–1352.

Lazarovici C.M., Lazarovici G. (2007): The architecture of the Neolithic and Copper Age period in Romania. The Copper Age period, Trinitas, Iași, pp. 399–482.

Livingstone Smith A. (2001): Bonfire II: The Return of Pottery Firing Temperatures. *Journal of Archaeological Science*, **28**, 991–1003.

Luca S.A. (2001): Aşezări neolitice pe valea Mureşului (II). Noi cercetări arheologice la Turdaş-Luncă. Campaniile anilor 1992-1995. În: BMA 17. Bucureşti, 210 p.

Luca S.A. (2009): Issues in defining the Foeni-Mintia Cultural-Group in Transylvania. In *Itinera Praehistorica. Studia in honorem magistri Nicolae Ursulescu quinto et sexagesimo anno* (V. Cotiugă, F.A. Tencariu, G. Bodi, eds.), Ed. Universității "A. I. Cuza" Iași, pp. 199–210.

Luca S.A., Roman C., Diaconescu D. (2004): Archaeological research in Cauce Cave, vol. I., Ed. Economică, 288 pp. (in Romanian).

Maggetti M. (1982): Phase analysis and its significance for technology and origin. In *Archaeological ceramics* (Olin JS, Franklin AD eds). Smithsonian Institute Press, Washington D.C., pp. 121–133.

Maggetti M. (2001): Chemical analyses of ancient ceramics: What for?, *Chimia*, **55**, 923–930.

Maggetti M., Neururer C., Ramseyer D. (2011): Temperature evolution inside a pot during experimental surface (bonfire) firing. *Applied Clay Science*, **53**, 500–508.

Manzoni S., Vico G., Katul G., Fay P.A., Polley W., Palmroth S., Porporato A. (2011): Optimizing stomatal conductance for maximum carbon gain under water stress: a meta-analysis across plant functional types and climates. *Functional Ecology*, **25**, 456–467.

Margaritelli G., Vallefuoco M., Di Rita F., Capotondi L., Bellucci L.G., Insinga D D., Petrosin, P., Bonomo S., Cacho I., Cascella A., Ferraro L., Florindo F., Lubritto C, Lurcock P.C., Magri D., Pelosi N., Rettori R., Lirer F. (2016): Marine response to climate changes during the last five millennia in the central Mediterranean Sea. *Global Planetary Change*, **142**, 53–72

Marincaș V., Nuțu A., Gheorghiță C. (1969): Moluşte tortoniene de la Popeşti-Hunedoara, în colecţia Muzeului Judeţean Deva. *Sargetia*, **VI**, 213–221.

Maritan L. (2004): Archaeometric study of Etruscan–Padan type pottery from the Veneto region: petrographic, mineralogical and geochemical-physical characterization. *European Journal of Mineralogy*, **16**, 297–307.

Maritan L., Angelini I., Artioli G., Mazzoli C., Saracino M. (2009): Secondary phosphates in the ceramic materials from Frattesina (Rovigo, north-eastern Italy). *Journal of Cultural Heritage*, **10**, 144–151.

Masi A., Sadori L., Baneschi I., Siani A.M., Zanchetta G. (2012): Stable isotope analysis of archaeological oak charcoal from eastern Anatolia as a marker of mid-Holocene climate change. *Plant Biology*, **15**, 83–92.

Masi A., Sadori L., Baneschi I., Siani A.M., Zanchetta G. (2013): Stable isotope analysis of archaeological oak charcoal from eastern Anatolia as a marker of mid-Holocene climate change. *Plant Biolo*gy, **15**, 83–92.

Mavridis F., Jensen J. T., Kormazopoulou L. (2013): Introduction. Stable spaces and changing perception: cave archaeology in Greece. In *Stable Places and Changing Perceptions: Cave Archaeology in Greece* (Mavridis F., Jensen J.T. eds.), British Archaeological Reports International, pp. 1–16.

Mazzucato E., Artioli G., Gualtieri A. (1999): High temperature dehydroxylation of muscovite-$2M_1$: a kinetic study by in situ XRPD. *Physics and Chemistry of Minerals*, **26**, 375–381.

Medeghini L., Nigro L. (2017): Khirbet al-Batrawy ceramics: a systematic mineralogical and petrographic study for investigating the material culture. *Periodico di Mineralogia*, **86**, 19–35.

Meldau R., Robertson H.S. (1953): Thermal decomposition of dolomite. *Nature*, **172**, 998–999.

Mentzer S.M. (2017): Rockshelter settings. In: *Encyclopedia of Geoarchaeology* (Gilbers A. ed). Encyclopedia of Earth Sciences Series. Springer, Dordrecht, pp. 725–743.

Mercader J., Garcia-Heras M., Gonzalez-Alvarez I. (2000): Ceramic tradition in the African forest: characterisation analysis of ancient and modern pottery from Ituri, D.R. Congo. *Journal of Archaeological Science*, **27**, 163–182.

Micu D.M., Dumitrescu A., Cheval S., Birasn M.-V. (2015): Conclusions. In: *Climate of the Romanian Carpathians*. Springer Atmospheric Sciences. Springer, Cham, pp. 207–210.

Molera J., Pradell T., Vendrell-Saz M. (1998): The colours of Ca-rich ceramic pastes: origin and characterization. *Applied Clay Science*, **13**, 187–202.

Murad E., Wagner U. (1996): The thermal behavior of an Fe-rich illite. *Clay Minerals*, **31**, 45–52.

Mureşan M., Mureşan G., Kräutner H.G. (1980): *Geological map of Romania, 1:50000, Hunedoara Sheet*. Geological and Geophysical Institute, Bucharest.

Nemes D.F. (1888): Ujabb adatok a bujturi mediterrán rétegek faunájának ismeretéhez. *Orv. terta. tud. Értesítő.*, **XIII**, 19–32.

Nodari L., Marcuz E., Maritan L., Mazzoli C., Russo U. (2007): Hematite nucleation and growth in the firing of carbonate-rich clay for pottery production. *Journal of the European Ceramic Society*, **27**, 4665–4673.

O'Leary M.H., Madhavan S., Paneth P. (1992): Physical and chemical basis of carbon isotope fractionation in plants. *Plant, Celt and Environment*, **15**, 1099-1104.

Onac B.P., Constantin S., Lundberg J., Lauritzen S.-E. (2002): Isotopic climate record in a Holocene stalagmite from Urșilor Cave (Romania). *Journal of Quaternary Science*, **17**(4), 319–327.

Onac B.P., Forray F.L., Wynn J.G., Giurgiu A.M. (2014): Guano-derived $\delta^{13}C$-based paleohydroclimate record from Gaura cu Muscă Cave, SW Romania. *Environmental Earth Sciences*, **71**, 4061–4069.

Osmond C.B., Allaway W.G., Sutton B.G., Troughton J.H., Queiroz O., Liittge U., Winter K. (1973): Carbon isotope discrimination in photosynthesis of CAM plants. *Nature*, **246**, 41–42.

Perry C.A., Hsu, K.J. (2000): Geophysical, archaeological, and historical evidence support a solar-output model for climate change. *Proceedings of the National Academy of Sciences*, **97**(23), 12433–12438.

Poole I., Braadbaart, F., Boon J.J., van Bergen P.F. (2002): Stable carbon isotope changes during artificial charring of propagules. *Organic Geochemistry*, **33**, 1675–1681.

Quinn P., Day P.M. (2007): Ceramic micropalaeontology: the analysis of microfossils in ancient ceramics. *Journal of Micropalaeontology*, **26**, 159–168.

Raczky P., Siklósi Z. (2013): Reconsideration of the Copper Age chronology of the eastern Carpathian Basin: a Bayesian approach. *Antiquity*, **87**, 555–573.

Rat'ko A.I., Ivanets A.I., Kulak A.I., Morozov E.A., Sakhar I.O. (2011): Thermal decomposition of natural dolomite. *Inorganic Materials*, **47**(12), 1372–1377.

Reimer P.J., Bard E., Bayliss A., Beck J.W., Blackwell P.G., Bronk Ramsey C., Buck C.E., Cheng H., Edwards R.L., Friedrich M., Grootes P.M., Guilderson T.P., Haflidason H., Hajdas I., Hatté C., Heaton T.J., Hoffmann D.L., Hogg A.G., Hughen K.A., Kaiser K.F., Kromer B., Manning S.W., Niu M., Reimer R.W., Richards D.A., Scott E.M., Southon J.R., Staff R.A., Turney C.S.M., van der Plicht J. (2013): IntCal13 and Marine13 radiocarbon age calibration curves 0-50,000 years cal BP. *Radiocarbon*, **55 (**4), 1869–1887.

Roman P. (1976): The Coţofeni culture. *Biblioteca de Arheologie*, **XXVI**, Editura Academiei Bucharest, 215 pp.

Roman C., Diaconescu D., Luca S.A. (2000): Archaeological research in Cerișor Cave No. 1 (Great Cave) (Leleșe village, Hunedoara County). *Acta Musei Corvinensis*, **6**, 7–59 (in Romanian.

Rodriguez-Navarro A., Cultrone G., Sanchez-Navas A., Sebastian E. (2003): TEM study of mullite growth after muscovite breakdown. *American Mineralogist*, **88**, 713–724.

Rusu A. (1998): Marcus Statius Priscus la Germisara. *Sargetia*, **XXI-XXIV** (1988-1991), 653–656.

Rutter J.B. (1975): Ceramic evidence for northern intruders in Southern Greece at the beginning of the Late Helladic IIIC Period. *American Journal of Archaeology*, **79**(1), 17–32. https://doi.org/10.2307/503336

Schirrmacher J., Kneisel J., Knitter D., Hamer W., Hinz M., Schneider R.R., Weinelt M. (2020): Spatial patterns of temperature, precipitation, and settlement dynamics on the Iberian Peninsula during the Chalcolithic and the Bronze Age. *Quaternary Science Reviews*, **233**, 106220.

Scott A.C., Damblon F. (2010): Charcoal: Taphonomy and significance in geology, botany and archaeology. *Palaeogeography, Palaeoclimatology, Palaeoecology*, **291**, 1–10.

Shepard A.O. (1956): Ceramics for the Archaeologist. Carnegie Institute, Washington, DC, USA, 414 pp.

Silva L.C., Horwath W.R. (2013): Explaining global increases in water use efficiency: why have we overestimated responses to rising atmospheric CO_2 in natural forest ecosystems? *PLoS ONE*, **8** (1), e53089.

Spasić M. (2010): Coţofeni communities at their southwestern frontier and their relationship with Kostolac population in Serbia. *Dacia N.S.*, **54**,157–175.

Sztancs D.M., Beldiman C., Ciută M.M. (2005): Podoabe din materii dure animale aparţinând culturii Coţofeni descoperite recent în Transilvania. *Revista Bistriţei*, **XIX**, 31–49.

Tanțău I., Reille M., de Beaulieu J.-L., Fărcaș S. (2006): Late Glacial and Holocene vegetation history in the southern part of Transylvania (Romania): pollen analysis of two sequences from Avrig. *Journal of Quaternary Science*, **21**, 49–61.

Tanțău I., Grindean R., Panit A., Diaconu A., Fărcaș S. (2016): Paleoenvironmental reconstructions since 5000 BC. In Landscape Archaeology on the Northern Frontier of the Roman Empire at Porolissum (Opreanu C.H., Lăzărescu V.-A., eds.). pp. 153–164.

Thér R. (2004): Experimental pottery firing in closed firing devices from the Neolithic – Hallstatt period in Central Europe. *EuroREA*, **1**, 35–82.

Thér R. (2014): Identification of pottery firing structures using the thermal characteristics of firing. *Archaeometry*, **56**, 78–99.

Tincu S. (2015): The archaeological researches from Hunedoara. Considerations regarding rultural and cronological framing of the discoveries (in Romanian). *Analele Banatului, S.N., Arheologie – Istorie*, **XXIII**, 63–87.

Tiwari M., Singh A.K., Sinha D.K. (2015): Stable Isotopes: Tools for understanding past climatic conditions and their applications in chemostratigraphy. In Chemostratigraphy, Concepts, Techniques, and Applications (Ramkumar M., ed.), Elsevier, pp. 65-92.

Trindade M.J., Dias M.I., Coroado J., Rocha F. (2009): Mineralogical transformations of calcareous rich clays with firing: a comparative study between calcite and dolomite rich clays from Algarve, Portugal. *Applied Clay Science*, **42**, 345–355.

Turekian V.C., Macko S., Ballentine D., Swap R.J., Garstang M. (1998): Causes of bulk carbon and nitrogen isotopic fractionations in the products of vegetation burns: laboratory studies. *Chemical Geology*, **152**, 181–192.

Turney C.S.M., Wheeler D., Chivas A.R. (2006): Carbon isotope fractionation in wood during carbonization. *Geochimica et Cosmochimica Acta*, **70**, 960–964.

Van Klinken G.J., Van Der Plicht H., Hedges R.E.M. (1994): Bond $^{13}C/^{12}C$ ratios reflect (palaeo-climatic variations. *Geophysical Research Letters,* **21** (6), 445 –448.

Velde B., Druc C.I. (1999): Archaeological Ceramic Materials. Origin and Utilization. Springer, Berlin, Germany, 299 pp.

Wagner T., Magill C.R., Herrle J.O. (2018): Carbon Isotopes. In: *Encyclopedia of Geochemistry* (W.M. White ed.*)*, Encyclopedia of Earth Sciences Series. Springer, Cham, pp. 194-204.

Weiss H. (2016): Global megadrought, societal collapse and resilience at 4.2-3.9 ka BP across the Mediterranean and west Asia. *Pages Magazine,* **24** (2), 62–63.

Wentworth C.K. (1922): A scale of grade and class terms for clastic sediments. *The Journal of Geology*, **30** (5), 377–392.

Zágoršek K., Silye L., Szabó B. (2008): New Bryozoa from the Sarmatian (Middle Miocene deposits of the Cerna-Strei Depression, Romania). *Studia Universitatis Babes-Bolyai, Geologia*, **53** (1), 25–29.

Websites:

www.carpatclim-eu.org